Baryon-baryon components in the deuteron as quark-exchange currents

L. Ya. Glozman[1,2] and E. I. Kuchina[2]
[1]Institute of Theoretical Physics, University of Tuebingen, Auf der Morgenstelle 14, D-72076 Tuebingen, Germany
[2]Alma-Ata Power Engineering Institute, Kosmonavtov 126, 480013 Alma-Ata, Kazakhstan
(Received 19 July 1993)

We systematically study the $NN \to$baryon + baryon quark-exchange terms. The effective numbers for the different baryon-baryon components in the deuteron are calculated.

PACS number(s): 24.85.+p, 13.75.Cs, 12.39.Pn

I. INTRODUCTION

One would think that due to the well-established three-quark structure of baryons one should expect some manifestations of possible six-quark structures in few-nucleon systems. But comparison of the deuteron electromagnetic form factors and tensor polarization at quite high momentum transfer with the quark [1,2] and the usual NN potential description shows that there is no room for qualitative quark effects which are not reduced to the usual NN picture in these observables.

Let us trace back in a short way the origin of this situation. The small amplitude of the deuteron wave function at small distances, which is a result of the repulsion in the usual NN phenomenology, was easily explained through the destructive interference of the quark configurations s^6 and s^4p^2 [1,3,4]. Indeed, microscopic calculations [3] have shown that the superposition of all excited quark configurations with different spatial $[f]_x$ and color-spin $[f]_{CS}$ (or spin-isospin) symmetries in the s^4p^2-s^52s shell can be presented as

$$\sum_{\alpha=[f]_x,[f]_{CS}} C_\alpha |(s^52s - s^4p^2)\alpha\rangle_{\rm TISM}$$

$$= -\gamma\sqrt{\tfrac{405}{410}}\hat{A}\{N(1,2,3)N(4,5,6)\varphi_{2s}(\mathbf{r})\}_{ST=10} + \text{small components}, \quad (1)$$

where the abbreviation TISM means the translationally invariant shell model, i.e., an exclusion of nonphysical center-of-mass oscillations. In this expression $\hat{A}$ is the quark antisymmetrizer,

$$\hat{A} = \frac{1}{\sqrt{10}}(1 - 9\hat{P}^{CSTX}_{36}), \quad (2)$$

and $\varphi_{nl} \equiv \varphi_{nlm}(\mathbf{r}/\sqrt{\frac{2}{3}}b)$ is a harmonic oscillator function with n excitation quanta; i.e., $\varphi_{2s}(\mathbf{r})$ is a two-quantum function with a node at $r = b \simeq 0.5$–0.6 fm. The coefficient γ determines the dynamical weight of the nodal $\hat{A}\{NN\varphi_{2s}\}$ component in the two-nucleon system.

On the other hand, the nonexcited six-quark configuration s^6 can be identically rewritten as

$$|s^6\rangle_{\rm TISM} = \sqrt{\tfrac{9}{10}}\hat{A}\{N(1,2,3)N(4,5,6)\varphi_{0s}(\mathbf{r})\}. \quad (3)$$

The full six-quark wave function at small distances is a destructive superposition of the nonexcited (3) and excited (1) six-quark components [1,3,4], so that this full wave function is analogous to the resonating group method (RGM) wave function [2,5,6]

$$\psi^d(1,\ldots,6) = \hat{A}\{N(1,2,3)N(4,5,6)\chi(\mathbf{r})\}, \quad (4)$$

where, at $r \leq 1$ fm,

$$\chi(\mathbf{r}) = \beta\sqrt{\tfrac{9}{10}}\varphi_{0s}(\mathbf{r}) - \gamma\sqrt{\tfrac{405}{410}}\varphi_{2s}(\mathbf{r}) + \text{small terms}, \quad (5)$$

being very small at $r \leq 0.5$–0.6 fm. Here β determines the weight of the s^6 components in the deuteron, $\beta^2 = 2$–$3.5\,\%$.

The difference between the microscopic quark description of the $2N$ system at small energies and the usual phenomenological one lies practically only in the presence of the quark antisymmetrizer $\hat{A}$ in expression (4) [of course, up to some distinction of $\chi(\mathbf{r})$ in (4) from the phenomenological NN wave functions].

The presence of the quark antisymmetrizer means the presence of the quark-exchange terms of Figs. 1(b)–1(e) in two-nucleon dynamics in addition to the usual ones of Fig. 1(a). Just these quark-exchange terms in combination with the color-exchange quark-quark forces provide the repulsive-core-like behavior of $\chi(\mathbf{r})$ at small distances in the RGM representation (4) [5,6].

The quark-exchange terms lead to the quark-exchange current (QEC) contribution of Fig. 2 in the deuteron electromagnetic form factors, tensor polarization, etc. [2,7]. But the QEC contribution is small compared to the conventional terms.

This smallness is quite understandable. First, the exchange terms are important at small distances, but the NN pair in the deuteron is dominantly at intermediate and large distances. Second, $\chi(\mathbf{r})$ in (4) dies out when penetrating into the "core zone." The third reason is the small value of the spin-isospin quark-exchange contribution in $NN \to NN$ channel, $C^{NN\to NN}_{ST=10} = -\frac{1}{27}$.[1]

[1]Strictly speaking, the first two diagrams of Fig. 2 comprise not only the $NN \to NN$ quark-exchange contribution but in addition the $NN \to N^*N$ quark-exchange contributions with subsequent deexcitation $\gamma^* + N^* \to N$. But these contributions are also determined by the small exchange factors.

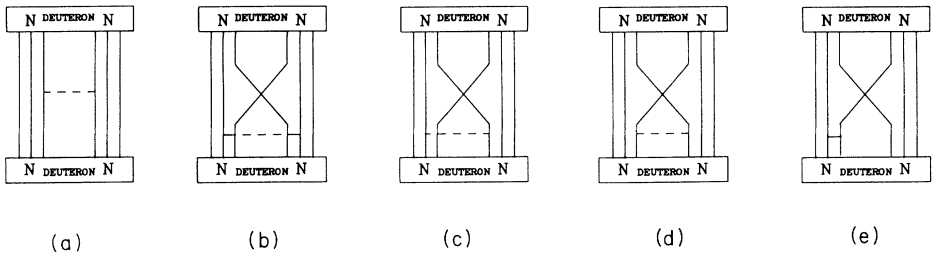

FIG. 1. Irreducible blocks defining the two-nucleon dynamics.

We would like to mention already here that the same factor for the $NN \to \Delta\Delta$ transition is one order of magnitude larger, $C_{ST=10}^{NN\to\Delta\Delta} = \frac{4\sqrt{5}}{27}$. It is essential that this factor be dynamically independent as far as it is determined only by the spin-isospin parts of N and Δ $3q$ wave functions. So we should expect in the case of the $NN \to \Delta\Delta$ transition a substantially larger QEC contribution than for $NN \to NN$.

In our previous papers [8,9], we have pointed out a new possibility to see and study the deuteron six-quark structure. Namely, because of the quark antisymmetrizer the six-quark wave function (4) contains not only the nucleon-nucleon component, but also a lot of other "baryon-baryon components," such as $\Delta\Delta, NN^*, N^*N^*, \ldots$.[2]

We have suggested there the $^2\mathrm{H}(e,e'p)\Delta$ and $^2\mathrm{H}(e,e'p)N^*$ reactions at CEBAF energies to make all these baryon-baryon components visible. In these papers the shell-model expansion [including s^6 and s^4p^2-s^52s shells; see (1)–(3)] of the function (4) at small range as long as the fractional parentage technique were used to estimate the spectroscopic factors for a few baryon-baryon components in the deuteron.

We should stress here that all these "baryon-baryon components" are in essence the quark-exchange terms of Fig. 3(a) and they are connected only with the six-quark region (the region of the nucleon overlap). But in addition there are baryon-baryon components at a little larger distances $r < 1.5$–2 fm which are determined by the usual meson-exchange dynamics between two "point-like" baryons [Fig. 3(b)].

In principle, both these mechanisms are coherent. In the Ref. [10] we have taken into account both the "quark-exchange" and the "meson-exchange" contributions when describing the virtual $d \to \Delta\Delta$ disintegration amplitude. It was shown that the quark-exchange mechanism dominates very much over the meson-exchange one. So in any process with one of the Δ as a spectator, for instance, in $^2\mathrm{H}(e,e'p)\Delta$ with $e + \Delta \to e' + p$ being the basic reaction, we shall see the quark-exchange contribution, i.e., the six-quark structure of the deuteron.

One of the old experiments $\gamma + d \to \Delta + x$ [11] showed the 3% of the $\Delta\Delta$ component which is in full agreement with our six-quark results [9,10]. That time only the usual meson-exchange mechanism for the $\Delta\Delta$ component in the deuteron was known [12], and the upper limit for $\Delta\Delta$ component in realistic calculations was less than 1%. Moreover, there was a good deal of skepticism concerning the old experiments with Δ as a spectator due to the final-state interaction and other mechanisms of Δ creation not connected with the preexisting $\Delta\Delta$ component in the deuteron [13]. But we should stress again that all that skepticism was based on the usual meson-exchange dynamics.

Now with a new generation of electron accelerators such as CEBAF or ELSA it is possible to study the exclusive $^2\mathrm{H}(e,e'p)\Delta, N^*$ reactions when the outgoing proton is very fast, $E_p > 1$ GeV, and the N^* spectator is very slow, practically at rest (or, better, moving in a backward direction). In this case the final-state interaction and Δ, N^* creation on one of the nucleons are suppressed and we shall see, probably, the quark-exchange currents.

This paper is the next one in series devoted to the quark description of baryon-baryon components in the deuteron and processes $^2\mathrm{H}(e,e'p)\Delta, N^*$ [8–10]. In this paper we systematically study the quark-exchange terms in the deuteron forming different baryon-baryon components. In contrast to our previous papers [8,9], we do not use the shell-model expansion of the deuteron six-quark wave function. We calculate all the quark-exchange terms directly from the function (4). This means that we include not only the s^6 and s^4p^2–s^52s shell configurations such as in [8,9], but all the higher ones. In some cases, for instance, for the $N(1520)N(1520)$, $N(1520)N(1535)$, ... components this is quite important.

We increase very much the number of different baryon-baryon components being under consideration and find some new ones which are essential.

The plan of the paper is the following. In Sec. II we discuss the definition of the virtual disintegration ampli-

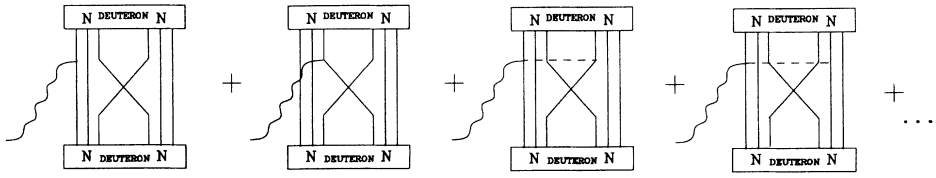

FIG. 2. Quark-exchange currents in the deuteron electromagnetic form factors.

[2]One should mention that the idea about $\Delta\Delta$, NN^*, . . . components in the deuteron six-quark wave function was discussed first in Refs. [29,30], but that time the six-quark structure of the deuteron at small range was not known.

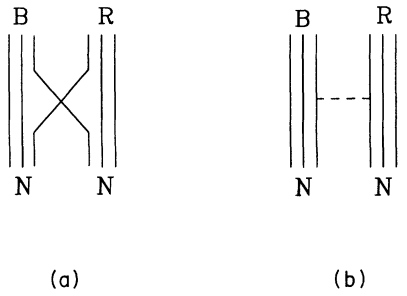

FIG. 3. (a) Quark-exchange term forming the non-nucleon baryon-baryon component; (b) standard meson-exchange $NN \to BR$ transition potential.

tude and the definition of the effective number for a given baryon-baryon component in the deuteron. We compare this approach with the usual Fock description. Section III is devoted to the three-quark basis for the baryon wave function. In Sec. IV we describe the structure of the quark-exchange matrix element. After that, in Secs. V–VII we present the effective numbers for different "quark-exchange" baryon-baryon components in the deuteron.

II. SOME DEFINITIONS

Let us consider the direct process depicted in Fig. 4 and compare the usual description using structureless baryons with the microscopic description on the quark level.

In the first case the deuteron wave function is presented as a Fock column

$$\psi_d = \begin{pmatrix} \psi_{NN} \\ \psi_{\Delta\Delta} \\ \psi_{NN^*} \\ \cdots \end{pmatrix}, \tag{6}$$

with a norm condition

$$\langle \psi_d | \psi_d \rangle = 1. \tag{7}$$

Here the norm of each row is a probability for the given component. The full probability is unity.

The electromagnetic current describing the spectator diagram of Fig. 4 in the nonrelativistic approach is

$$j^{\nu}_{d\to RC} \sim \sqrt{2} \sum_B \psi_{BR}(\mathbf{K}_R) j^{\nu}_{B\to C}, \tag{8}$$

where the factor $\sqrt{2}$ is due to antisymmetrization in the final state [we assume that each row in (6) is antisymmetric with respect to baryon transposition].

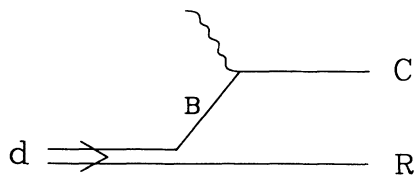

FIG. 4. Spectator diagram for the process $\gamma + d \to C + R$.

In the microscopic six-quark approach one has instead of the Fock column (6) the six-quark deuteron wave function $\psi_d(1,2,\ldots,6)$ which depends on five internal Jacobi coordinates and is normalized again to unity:

$$\langle \psi_d(1,2,\ldots,6) | \psi_d(1,2,\ldots 6) \rangle = 1. \tag{9}$$

There were debates about how to define the relative motion wave function of the given baryon-baryon component BR in the microscopic approach [4,14]. But nevertheless the answer is trivial. The relative motion wave function for the baryons B and R at small range, i.e., where the processes of quark exchange between the three-quark clusters are essential, strictly speaking, does not exist.

To understand this it is enough to remember that the two-system relative motion is described by the wave function only if these systems are well defined. More concretely, only if there are well-defined boundary conditions for both clusters $B(1,2,3)$ and $R(4,5,6)$. Only in this case one could split up the Schrödinger equation for six particles into Schrödinger equations of the internal motion of each cluster and the relative motion Schrödinger equation. Here the full six-quark wave function could be presented as a product of the internal baryon wave functions and the relative motion wave function.

Of course, at large distances these conditions are fulfilled. But at small range due to the quark permutations each of the baryons loses its individuality. So here the relative motion wave function does not exist in principle [one should not mix the trial function $\chi(\mathbf{r})$ in (4) with the relative motion wave function; only at large and intermediate distances does $\chi(\mathbf{r})$ coincide with the relative motion wave function].

That is why there is a problem of the unitary off-shell ambiguity in the usual RGM interpretation of the function

$$\bar{\chi}(\mathbf{r}) = \int N^{1/2}(\mathbf{r},\mathbf{r}')\chi(\mathbf{r}')d\mathbf{r}' \tag{10}$$

as a relative motion wave function instead of $\chi(\mathbf{r})$ [14]. Here the $N(\mathbf{r},\mathbf{r}')$ is the nonlocal norm kernel [see below, (21)].

In the microscopic approach, one should solve the problem only with the full six-quark wave function on the level of matrix elements. Of course, the matrix element for the given transition is a probability amplitude.

Let us look at the structure of the matrix element corresponding to Fig. 4. For details we refer readers to Ref. [9] and present here only the points which are essential for understanding.

Consider an interaction of external field with the individual constituent quark. In this case,

$$j^{\nu}_{d\to RC} = \sum_{k=1}^{6} \int \prod_{i=1}^{6} d\mathbf{r}_i e^{i\mathbf{q}\cdot\mathbf{r}_k} \{\psi^*_{RC}(1,2,\ldots,6) \times \hat{j}^{\nu}(k)\psi_d(1,2,\ldots,6)\}. \tag{11}$$

With the momentum $\mathbf{k}_c$ being very large and $\mathbf{k}_R \simeq 0$, our matrix element (11) in the plane wave approximation is

$$j^{\nu}_{d\to RC} = \int \prod_{i=1}^{6} d\mathbf{r}_i e^{-i\mathbf{k}_C\cdot\mathbf{r}_C} e^{-i\mathbf{k}_R\cdot\mathbf{r}_R} \times\sqrt{\frac{6!}{3!3!}}\varphi_C(1,2,3)\varphi_R(4,5,6) \times\sum_{k=1}^{3} e^{i\mathbf{q}\cdot\mathbf{r}_k}\hat{j}^{\nu}(k)\psi_d(1,2,\ldots,6), \quad (12)$$

where

$$\mathbf{r}_C = \frac{\mathbf{r}_1+\mathbf{r}_2+\mathbf{r}_3}{3}, \quad \mathbf{r}_R = \frac{\mathbf{r}_4+\mathbf{r}_5+\mathbf{r}_6}{3}, \quad \mathbf{r} = \mathbf{r}_C - \mathbf{r}_R, \quad (13)$$

and $\varphi_C(1,2,3)$ and $\varphi_R(4,5,6)$ are internal baryons wave functions. The factor $\sqrt{\frac{6!}{3!3!}}$ appears in (12) due to the identity of quarks in the final state.

For the sake of convenience, let us insert into the matrix element (12) just after the current operator $\hat{j}(k)$ the unity

$$\sum_{B,M_B}\int d\mathbf{k}_B|\varphi_B(1,2,3)\mathbf{k}_B\rangle\langle\varphi_B(1,2,3)\mathbf{k}_B| = 1, \quad (14)$$

where the summation is carried out over all the possible states of $3q$ cluster B, its spin and spin projection M_B, etc., and $\mathbf{k}_B$ is the cluster center-of-mass momentum.

As a result, we derive an expression such as (8) but with the microscopically determined amplitude instead of that in (8). Namely,

$$\psi^d_{BR}(\mathbf{K}_R) = \frac{1}{(2\pi)^{3/2}}\int d\mathbf{r}\, e^{i\mathbf{K}_R\cdot\mathbf{r}}\psi^d_{BR}(\mathbf{r}), \quad (15)$$

$$\psi^d_{BR}(\mathbf{r}) = \left(\frac{6!}{3!3!2}\right)^{1/2}\langle\varphi_B(1,2,3)\varphi_R(4,5,6)|\psi_d(1,2,\ldots,6)\rangle,$$

and

$$j^{\nu}_{B\to C} = \sum_{k=1}^{3}\int\prod_{i=1}^{3} d\mathbf{r}_i e^{i\mathbf{q}\cdot\mathbf{r}_k} e^{-i\mathbf{K}_C\cdot\mathbf{r}_C}\varphi_C(1,2,3)\hat{j}^{\nu}(k)\varphi_B(1,2,3)e^{-i\mathbf{K}_R\cdot\mathbf{r}_C}. \quad (16)$$

The last expression (16) is the matrix element of the hadron current for the process $\gamma^* + B \to C$, where $-\mathbf{K}_R$ is the momentum of the initial virtual cluster B and $\mathbf{K}_C$ is the final momentum of particle C.

The virtual disintegration amplitude (15) appears in the microscopic matrix element instead of corresponding Fock row. But we stress again that this is not, strictly speaking, the relative motion wave function. This amplitude comprises both the direct and quark-exchange terms of Fig. 5.

The effective number for the given baryon-baryon component,

$$N^d_{BR} = \frac{1}{2J_d+1}\sum_{M_BM_RM_d}\int|\psi^d_{BR}(\mathbf{r})|^2 d\mathbf{r} = \frac{1}{2J_d+1}\sum_{M_BM_RM_d}\int|\psi^d_{BR}(\mathbf{K}_R)|^2 d\mathbf{K}_R \quad (17)$$

is connected with the spectroscopic factor S^d_{BR} for the same component as

$$N^d_{BR} = \tfrac{1}{2}S^d_{BR}. \quad (18)$$

The sum of the effective numbers N^d_{BR} over all possible three-quark clusters R and B is not unity. It depends on the full six-quark wave function.

For example, in the limit, where the size of each cluster $B(1,2,3)$ and $R(4,5,6)$ approaches zero, the sum mentioned above is unity and the amplitude (15) is the Fock relative motion wave function (there is no contribution of all the exchange diagrams of Fig. 5 in this limit).

In the opposite limit, where there is no clusterization in the six-quark wave function $\psi_d(1,2,\ldots,6)$ and this function is a shell-model wave function, one has $\sum_{B,R} N^d_{BR} = \frac{6!}{3!3!2}$ (including also all the color clusters). This normalization is due to the orthonormality of the

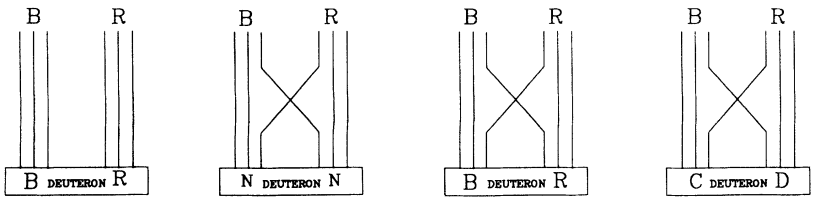

FIG. 5. Direct and quark-exchange contributions into the virtual disintegration amplitude $d \to B + R$.

fractional paraentage expansion.

In reality, the six-quark deuteron wave function is a well-clustered function [at $r \geq 2$ fm this function is only $\varphi_N \varphi_N \chi_{NN}(\mathbf{r})$] and the sum condition is

$$\sum_{B,R} N_{BR}^{d} = 1 + \delta,$$

where $\delta \ll 1$ and depends on the microscopically derived wave function behavior at short distances.

One should mention that expressions such as (15) have been used in the theory of cluster knock-out from light nuclei for 20 years [15,16]. But unfortunately as applied to the baryon-baryon composition of the deuteron in paper [4] the authors tried to treat this quantity as a relative motion wave function with a typical RGM renormalization by the nonlocal norm operator, which, as was mentioned above, is not correct.

We should stress also that both expressions (8) and (11) use the one-body electromagnetic current (or any one-body operator) which is well known to be not conserved in a system of interacting particles. To provide the current conservation (the gauge invariance), we should add two-body exchange currents such as the third and fourth diagrams of Fig. 2 or use explicitly covariant formalism. In the case of the two-body operator acting on the quarks from the outgoing fast baryon, for example, 1 and 2, we have to modify only the expression (16) for the hadron current. But for the two-body operator acting on the quarks from the different clusters, for instance, 1 and 4, we would have a "distorted" amplitude instead of that in expression (15). So, strictly speaking, the amplitudes (15) are mainly applicable for the processes or kinematics where these two-body currents are not essential. This takes place at very nonsymmetrical kinematics (particle C being very fast and particle R being slow or, better, moving in a backward direction). In the opposite case, one should take into account these "distortions" explicitly.

On the contrary, the effective numbers are integral characteristics and they appear in the microscopic approach instead of the probabilities for the different baryon-baryon components. They reflect the nontrivial structure of the six-quark wave function. But we should remember that their definition is not relativistically covariant and that we deal here with the nonrelativistic six- and three-quark wave functions which provide only a qualitative picture.

In this paper we consider the function in form (4) as the proper six-quark deuteron wave function. So we deal only with the quark-exchange contribution into the disintegration amplitude (15) and effective numbers (17). (In the case of the NN component, there are both the direct and quark exchange-term contributions).

Let us turn now to the microscopic six-quark wave functions. In our calculations we have used two different six-quark deuteron wave functions (4).

The first has been developed in Ref. [10] with the microscopic six-quark Hamiltonian

$$H = 6m_q + \sum_{i=1}^{6} \frac{\mathbf{p}_i^2}{2m_q} - \frac{\mathbf{P}^2}{12m_q} + \sum_{i<j=1}^{6} V_{ij}. \tag{19}$$

This microscopic six-quark Hamiltonian includes, first, the quark-quark color-exchange potential which is responsible for the very-short-range phenomena and motivated in its form from the charmonium spectroscopy [17] (the so-called one-gluon-exchange potential (OGEP) with the effective strong coupling constant),

$$V_{ij}^{\mathrm{OGEP}} = \frac{\alpha_s}{4} \lambda_i^a \cdot \lambda_j^a \left\{ \frac{1}{r} - \frac{\pi}{m_q^2} \left(1 + \frac{2}{3} \boldsymbol{\sigma}_i \cdot \boldsymbol{\sigma}_j\right) \delta(\mathbf{r}) - \frac{1}{4m_q^2 r^3} \left(3\boldsymbol{\sigma}_i \cdot \mathbf{r} \boldsymbol{\sigma}_j \cdot \mathbf{r} - \boldsymbol{\sigma}_i \cdot \boldsymbol{\sigma}_j\right) - \frac{3}{m_q^2 r^3} \mathbf{r} \times \mathbf{p}_{ij} \cdot (\boldsymbol{\sigma}_i + \boldsymbol{\sigma}_j) \right\}, \tag{19'}$$

with $\alpha_s \simeq 0.36$–0.4. Second, the quark-confinement potential in the quadratic form

$$V_{ij}^{\mathrm{conf}} = -\lambda_i^a \cdot \lambda_j^a (a_c r^2 - C), \tag{19''}$$

which does not contribute to the baryon-baryon dynamics [5].

Both the interactions (19′) and (19″) along with the constituent quark mass $m_q \simeq \frac{1}{3} m_N$ (this mass evidently has some dynamical origin [18,19]) simulate stringlike and some part of the relativistic effects.

And finally the Hamiltonian (19) includes π and σ exchange on the quark level derived from the linear σ-model interaction Hamiltonian

$$H = g\bar{\Psi}(\sigma + i\boldsymbol{\pi}\boldsymbol{\tau}\gamma_5)\Psi \tag{19'''}$$

where Ψ corresponds to the constituent quark (the so-called chiral phase; in this chiral-invariant form it was introduced into the nucleon-nucleon dynamics on the quark level in Ref. [4]) with short-range cutoff via the monopole form factor in the effective quark-meson vertex

$$g \to g \left(\frac{\Lambda^2}{\Lambda^2 + \mathbf{k}^2}\right)^{1/2},$$

with $\Lambda = 4.2$ fm^{-1}, $m_\sigma = 2m_q$, and $g = \frac{3}{5}(m_q/m_N) g_{\pi N}$. One has a few reasons for the introduction of this chiral phase. First, because the nucleon-nucleon interaction is governed at intermediate and large distances by meson exchange, we need in the framework of the constituent quark model a direct pion-quark and sigma-quark coupling. Second, within the constituent quark model without the chiral phase interaction, it is difficult to obtain partially conserved axial current (PCAC). The third reason is that it is difficult to explain on the basis of the potentials (19′) and (19″) why the two-quantum nucleon excitation $N(1440)$ lies below the one-quantum excitations $N(1520)$ and $N(1535)$.

This calculation includes all irreducible blocks of Fig. 1. It should be mentioned that this type of $6q$ Hamiltonian allows one to describe qualitatively both the baryon spectrum including low-lying resonances and the two-nucleon system (NN phase shifts and the deuteron) [4,10,20,21].

The second wave function is a phenomenological one and has been developed on the basis of the Paris deuteron wave function. The purpose of the calculation with this

phenomenological wave function is only to estimate the value of possible deviations of the effective numbers.

We cannot use a phenomenological deuteron NN wave function in (4) as $\chi(\mathbf{r})$. In this case the full six-quark wave function (4) is not normalized to unity due to the quark-exchange terms. To correct this we renormalize the Paris wave function in accordance with

$$\chi(\mathbf{r}) = \int N^{-1/2}(\mathbf{r},\mathbf{r}')\chi^{\text{Paris}}(\mathbf{r}')d\mathbf{r}', \tag{20}$$

where $\hat{N}(\mathbf{r},\mathbf{r}')$ is the nonlocal norm operator,

$$\hat{N}(\mathbf{r},\mathbf{r}') = \delta(\mathbf{r}-\mathbf{r}') + \langle\{\varphi_N(1,2,3)\varphi_N(4,5,6)\}_{ST=10}\delta(\mathbf{r}-\mathbf{r}'')| - 9\hat{P}_{36}|\{\varphi_N(1,2,3)\varphi_N(4,5,6)\}_{ST=10}\delta(\mathbf{r}'-\mathbf{r}'')\rangle. \tag{21}$$

The exchange part of the norm operator (21) with the simple s^3 harmonic oscillator wave function for the nucleon (center-of-mass oscillations are removed) with the oscillator parameter b is

$$N^{\text{exch}}(\mathbf{r},\mathbf{r}') = \frac{1}{9}\left(\sqrt{\frac{3}{2}}\frac{1}{b}\right)^3\left(\frac{9}{8\pi}\right)^{3/2}\exp\left\{-\frac{15}{16b^2}\left(r^2+r'^2-\frac{6}{5}\mathbf{r}\cdot\mathbf{r}'\right)\right\}. \tag{22}$$

The exchange operator (22) has the oscillator functions $\varphi_{nlm}(\frac{\mathbf{r}}{\sqrt{2/3}b})$ as the eigenfunctions:

$$\int d\mathbf{r}'\, N^{\text{exch}}(\mathbf{r},\mathbf{r}')\varphi_{nlm}\left(\frac{\mathbf{r}'}{\sqrt{2/3}b}\right) = 3^{-(n+2)}\varphi_{nlm}\left(\frac{r}{\sqrt{2/3}b}\right),$$

where n is a number of excitation quanta.

We treat the power $-\frac{1}{2}$ of the norm operator in (20) as usual replacing the eigenvalues $1+3^{-(n+2)}$ by the $(1+3^{-(n+2)})^{-1/2}$ in the eigenstate representation.

In all our calculations, we use the quark oscillator parameter (the quark core radius of the nucleon) $b = 0.5$ fm.

III. BARYONS WAVE FUNCTIONS

For the nonstrange baryons, the fully antisymmetric three-quark state can be built as an inner product of the color singlet $[1^3]_C$ and spatial-spin-isospin $[3]_{XST}$ singlet representations

$$[1^3]_{CXST} = [1^3]_C \times [3]_{XST}.$$

In principle, there are two different types of notations for three-particle harmonic oscillator wave functions (center-of-mass oscillations are removed) in baryon spectroscopy [22,23] and in nuclear physics [translationally invariant shell model (TISM)] [24,15,16]. We prefer to use the second one which is based on the Elliot classification scheme and is used successfully not only for three-particle wave functions, but also for many-particle ones.

The spatial part of the TISM state is determined by the quantum numbers

$$|N(\lambda\mu)[f]L(r)\rangle,$$

where N is the number of the internal excitation quanta, $(\lambda\mu)$ the Elliot symbol which determines the harmonic oscillator SU(3) multiplet, L the internal orbital momentum, $[f]$ the Young scheme (pattern) defining the spatial permutation symmetry, and (r) is the Yamanouchi symbol which determines the row of the irreducible representation $[f]$ of the permutation group. The number of Yamanouchi symbols compatible with a given Young pattern is just the dimension of the given representation. The Yamanouchi symbol is uniquely connected with the Young tableau. [Do not mix the Young scheme (pattern) with the Young tableau. The last one is the Young scheme where the numbers are placed in each box [25].]

The fully symmetric spatial-spin-isospin part $[3]_{XST}$ is determined by the quantum numbers

$$|N(\lambda\mu)[f]LST\rangle$$

and is constructed as

$$|N(\lambda\mu)[f]LST\rangle = \frac{1}{\sqrt{\dim[f]}}\sum_{(r)}|N(\lambda\mu)[f]_X L(r)_X\rangle \times|[f]_{ST}ST(r)_{ST}\rangle, \tag{23}$$

where $|[f]_{ST}ST(r)_{ST}\rangle$ is the spin-isospin part with an ST Young pattern $[f]_{ST} = [f]_X \equiv [f]$ and the Yamanouchi symbols $(r)_{ST} = (r)_X \equiv (r)$. Here also

$$\dim[f] = \begin{cases} 1 & \text{if } [f] = [3];[1^3], \\ 2 & \text{if } [f] = [21]. \end{cases}$$

To be short we drop in (23) the projections M_L, M_S, and M_T. To get the wave function with full momentum $\mathbf{J} = \mathbf{L} + \mathbf{S}$, it is necessary to go to the coupled representation

$$|N(\lambda\mu)[f]LST:J\rangle = \sum_{M_L M_S} C^{JM_J}_{LM_L SM_S}|N(\lambda\mu)[f]LST\rangle, \tag{24}$$

where $C^{JM_J}_{LM_L SM_S}$ are the usual SU(2) Clebsch-Gordan coefficients.

Thus, for particles with $J^P, T = \frac{1}{2}^+, \frac{1}{2}$ ($N(939)$, $N(1440), N(1710), \dots$), there are five basis states within $N = 0, 2$ bands:

$$|N_0\rangle = |0(00)[3]0\tfrac{1}{2}\tfrac{1}{2}\rangle,$$
$$|N_1\rangle = |2(20)[3]0\tfrac{1}{2}\tfrac{1}{2}\rangle,$$
$$|N_2\rangle = |2(20)[21]0\tfrac{1}{2}\tfrac{1}{2}\rangle,$$
$$|N_3\rangle = |2(20)[21]2\tfrac{3}{2}\tfrac{1}{2}\rangle,$$
$$|N_4\rangle = |2(01)[111]1\tfrac{1}{2}\tfrac{1}{2}\rangle.$$

For particles with $J^P, T = \frac{3}{2}^+\frac{3}{2}$ ($\Delta(1232), \Delta(1600)$, $\Delta(1920), \dots$), there are four states with $N = 0, 2$:

$$|\Delta_0\rangle = |0(00)[3]0\tfrac{3}{2}\tfrac{3}{2}\rangle,$$
$$|\Delta_1\rangle = |2(20)[3]0\tfrac{3}{2}\tfrac{3}{2}\rangle,$$
$$|\Delta_2\rangle = |2(20)[3]2\tfrac{3}{2}\tfrac{3}{2}\rangle,$$
$$|\Delta_3\rangle = |2(20)[21]2\tfrac{1}{2}\tfrac{3}{2}\rangle.$$

For particles with negative parity $J^P, T = \frac{1}{2}^-$, $\frac{1}{2}(N(1535), N(1650), \dots)$, there are two basis states within the band with $N = 1$ and seven states with $N = 3$:

$$|N_1^{(-)}\rangle = |1(10)[21]1\tfrac{11}{22}\rangle,$$
$$|N_2^{(-)}\rangle = |1(10)[21]1\tfrac{31}{22}\rangle,$$
$$|N_3^{(-)}\rangle = |3(11)[21]1\tfrac{1}{2}\tfrac{1}{2}\rangle,$$
$$|N_4^{(-)}\rangle = |3(11)[21]1\tfrac{3}{2}\tfrac{1}{2}\rangle,$$
$$|N_5^{(-)}\rangle = |3(30)[3]1\tfrac{1}{2}\tfrac{1}{2}\rangle,$$
$$|N_6^{(-)}\rangle = |3(30)[21]1\tfrac{1}{2}\tfrac{1}{2}\rangle,$$
$$|N_7^{(-)}\rangle = |3(30)[21]1\tfrac{3}{2}\tfrac{1}{2}\rangle,$$
$$|N_8^{(-)}\rangle = |3(11)[21]2\tfrac{3}{2}\tfrac{1}{2}\rangle,$$
$$|N_9^{(-)}\rangle = |3(30)[111]1\tfrac{1}{2}\tfrac{1}{2}\rangle.$$

For the other particles, the basis states can be constructed analogously.

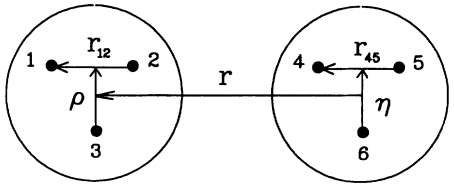

FIG. 6. Jacobi coordinates in the six-quark system.

All the necessary wave functions are presented in Appendix A.

One should mention that our phase definitions are not the same as in Ref. [22]. For example,

$$|^2 8(56', 0^+)\tfrac{1}{2}^+\rangle \equiv |8^2 S_S \tfrac{1}{2}^+\rangle = -|2(20)[3]0\tfrac{1}{2}\tfrac{1}{2}\rangle,$$
$$|^2 8(70, 0^+)\tfrac{1}{2}^+\rangle \equiv |8^2 S_M \tfrac{1}{2}^+\rangle = +|2(20)[21]0\tfrac{1}{2}\tfrac{1}{2}\rangle,$$
$$|^4 10(56', 0^+)\tfrac{3}{2}^+\rangle \equiv |10^4 S_S \tfrac{3}{2}^+\rangle = -|2(20)[3]0\tfrac{3}{2}\tfrac{3}{2}\rangle.$$

IV. STRUCTURE OF THE QUARK-EXCHANGE MATRIX ELEMENTS

Here we start with the expression (15) for the virtual disintegration amplitude,

$$\psi^d_{BR}(\mathbf{r}) = \sqrt{10}\langle\varphi_B^{J_B M_B}(1,2,3)\varphi_R^{J_R M_R}(4,5,6)|\psi_d(1,2,\dots 6)\rangle,$$

with fixed projections of particles B and R, and use the wave function (4) as the deuteron six-quark wave function. One has

$$\psi^d_{BR}(\mathbf{r}) = \chi(\mathbf{r})\delta_{B,N}\delta_{R,N} + (-9)\tfrac{1}{3}\langle\varphi_B^{J_B M_B}(1,2,3)\varphi_R^{J_R M_R}(4,5,6)|\hat{P}^{STX}_{36}|\{\varphi_N(1,2,3)\varphi_N(4,5,6)\chi(\mathbf{r})\}_{J_d=1M_d}\rangle, \tag{25}$$

where $\frac{1}{3}$ is the color-exchange factor,

$$\langle\{[1^3]_C \otimes [1^3]_C\}_{[2^3]_C}|\hat{P}^C_{36}|\{[1^3]_C \otimes [1^3]_C\}_{[2^3]_C}\rangle = \tfrac{1}{3}. \tag{26}$$

We consider only the S-wave component of $\chi(\mathbf{r})$. The quark-exchange contribution for the D wave is three orders of magnitude less than the one for the S wave.

We use the Jacobi coordinates of Fig. 6 and $|0(00)[3]0\frac{1}{2}\frac{1}{2}\rangle$ functions for the nucleons (s^3 harmonic oscillator wave function with the center-of-mass oscillations being removed). So one has

$$\{\varphi_N(1,2,3)\varphi_N(4,5,6)\chi(\mathbf{r})\}_{J_d=1M_d} = \varphi_{000}(\mathbf{r}_{12})\varphi_{000}(\mathbf{r}_{45})\varphi_{000}(\boldsymbol{\rho})\varphi_{000}(\boldsymbol{\eta})\chi_{L=0}(\mathbf{r})\{|[3]ST = \tfrac{1}{2}\tfrac{1}{2}\rangle \otimes |[3]ST = \tfrac{1}{2}\tfrac{1}{2}\rangle\}_{ST=10}. \tag{27}$$

As far as

$$\varphi_B^{J_B M_B}(1,2,3)\varphi_R^{J_R M_R}(4,5,6) = \sum_{\substack{m_B m_R \\ \mu_B \mu_R}} C^{J_B M_B}_{L_B m_B S_B \mu_B} C^{J_R M_R}_{L_R m_R S_R \mu_R} C^{M_R}_{L_R} \frac{1}{\sqrt{\dim[f_B]}} \frac{1}{\sqrt{\dim[f_R]}} \times \sum_{(r_B)(r_R)} |N_B(\lambda\mu)_B[f_B]L_B(r_B)\rangle|N_R(\lambda\mu)_R[f_R]L_R(r_R)\rangle \times|[f_B]S_B T_B(r_B)\rangle|[f_R]S_R T_R(r_R)\rangle, \tag{28}$$

the STX-exchange matrix element in the expression (25) can be decomposed into spatial and spin-isospin parts:

$$\langle\varphi_B^{J_B M_B}(1,2,3)\varphi_R^{J_R M_R}(4,5,6)|\hat{P}^{STX}_{36}|\{\varphi_N(1,2,3)\varphi_N(4,5,6)\chi(\mathbf{r})\}_{J_d=1M_d}\rangle$$
$$= \sum_{\substack{m_B m_R \\ \mu_B \mu_R \\ (r_B)(r_R)}} C^{J_B M_B}_{L_B m_B S_B \mu_B} C^{J_R M_R}_{L_R m_R S_R \mu_R} \frac{1}{\sqrt{\dim[f_B]}} \frac{1}{\sqrt{\dim[f_R]}} \langle[f_B]S_B\mu_B T_B t_B(r_B); [f_R]S_R\mu_R T_R t_R(r_R)|\hat{P}^{ST}_{36}|$$
$$\times\{|[3]ST = \tfrac{1}{2}\tfrac{1}{2}\rangle \otimes |[3]ST = \tfrac{1}{2}\tfrac{1}{2}\rangle\}_{ST=10}\langle N_B(\lambda\mu)_B[f_B]L_B m_B(r_B); N_R(\lambda\mu)_R[f_R]L_R m_R(r_R)$$
$$\times|\hat{P}^X_{36}|\varphi_{000}(\mathbf{r}_{12})\varphi_{000}(\mathbf{r}_{45})\varphi_{000}(\boldsymbol{\rho})\varphi_{000}(\boldsymbol{\eta})\chi_{L=0}(\mathbf{r})\rangle. \tag{29}$$

The operator $\hat{P}^X_{36}$ acts only on the functions $\varphi_{000}(\boldsymbol{\rho})$, $\varphi_{000}(\boldsymbol{\eta})$, and $\chi_{L=0}(\mathbf{r})$.

As far as both the $|N_B(\lambda\mu)_B[f_B]L_B(r_B)\rangle$ and the $|N_R(\lambda\mu)_R[f_R]L_R(r_R)\rangle$ are decomposed into products of the harmonic oscillator functions of the internal Jacobi coordinates (see Appendix A) and due to the orthogonality of $\varphi_{nlm}(\mathbf{r}_{12})$ and $\varphi_{000}(\mathbf{r}_{12})$, $\varphi_{nlm}(\mathbf{r}_{45})$ and $\varphi_{000}(\mathbf{r}_{45})$ for $nlm \neq 000$, the sum over (r_R) and (r_B) in (29) vanishes and the spatial part is reduced:

$$\langle N_B(\lambda\mu)_B[f_B]L_B m_B(r_B);\ N_R(\lambda\mu)_R[f_R]L_R m_R(r_R)|\hat{P}^X_{36}|\varphi_{000}(\mathbf{r}_{12})\varphi_{000}(\mathbf{r}_{45})\varphi_{000}(\boldsymbol{\rho})\varphi_{000}(\boldsymbol{\eta})\chi_{L=0}(\mathbf{r})\rangle$$

$$= \gamma^X_B\gamma^X_R \int \varphi^*_{N_BL_Bm_B}(\boldsymbol{\rho})\varphi^*_{N_RL_Rm_R}(\boldsymbol{\eta})\hat{P}^X_{36}\{\varphi_{000}(\boldsymbol{\rho})\varphi_{000}(\boldsymbol{\eta})\chi_{L=0}(\mathbf{r})\}d\boldsymbol{\rho}\,d\boldsymbol{\eta}, \quad (30)$$

where γ^X_B and γ^X_R are the orbital fractional parentage coefficients,

$$\gamma^X_B = \langle N_B(\lambda\mu)_B[f_B]L_B|0(00)[2]0, N_BL_B\rangle,$$

$$\gamma^X_R = \langle N_R(\lambda\mu)_R[f_R]L_R|0(00)[2]0, N_RL_R\rangle$$

(i.e., the weights of the components $\varphi_{000}(\mathbf{r}_{12})\varphi_{N_BL_Bm_B}(\boldsymbol{\rho})$ and $\varphi_{000}(\mathbf{r}_{45})\varphi_{N_RL_Rm_R}(\boldsymbol{\eta})$ in the functions $|N_B(\lambda\mu)_B[f_B]L_B(r_B)\rangle$ and $|N_R(\lambda\mu)_R[f_R]L_R(r_R)\rangle$, respectively). These coefficients can be easily extracted from the spatial parts in Appendix A.

To calculate the spatial exchange integral (30), we approximate the function $\chi_{L=0}(r)$ $[\chi_{L=0}(\mathbf{r}) = \chi_{L=0}(r)Y_{00}(\mathbf{r})]$ with high accuracy by the Gaussians

$$\chi_{L=0}(r) = \sum_k A_k e^{-\alpha_k r^2}. \quad (31)$$

In this case the integrals are calculated analytically,

$$\int \varphi^*_{N_BL_Bm_B}(\boldsymbol{\rho})\varphi^*_{N_RL_Rm_R}(\boldsymbol{\eta})\hat{P}^X_{36}\{\varphi_{000}(\boldsymbol{\rho})\varphi_{000}(\boldsymbol{\eta})e^{-\alpha_k r^2}Y_{00}(\hat{r})\}d\boldsymbol{\rho}\,d\boldsymbol{\eta}$$

$$= \sum_L C^{L,m_B+m_R}_{L_Bm_BL_Rm_R} I^L_{N_BL_B,N_RL_R}(r;\alpha_k)Y^*_{L,m_B+m_R}(\hat{r}). \quad (32)$$

In the expression (32) the summation is carried out over L with the same parity as $L_B + L_R$; for example, if $L_B = 1$ and $L_R = 2$, the possible values of L are $L = 1, 3$. The functions $I^L_{N_BL_B,N_RL_R}(r;\alpha_k)$ can be found in Appendix B.

In its turn the spin-isospin exchange matrix element in (29) is

$$\langle [f_B]S_B\mu_BT_Bt_B(r_B);\ [f_R]S_R\mu_RT_Rt_R(r_R)|\hat{P}^{ST}_{36}|\{|[3]ST = \tfrac{1}{2}\tfrac{1}{2}\rangle \otimes |[3]ST = \tfrac{1}{2}\tfrac{1}{2}\rangle\}_{ST=10}\rangle$$

$$= (-1)^{1/2+S_B+2T_B}\sqrt{2(2S_B+1)(2S_R+1)(2T_B+1)}C^{1M_d}_{S_B\mu_BS_R\mu_R}C^{00}_{T_Bt_BT_Rt_R}$$

$$\times \sum_{\substack{S_{12}=T_{12}=0,1\\ S_{45}=T_{45}=0,1}} \langle [f_B]S_BT_B|[2]S_{12}T_{12};\tfrac{1}{2}\tfrac{1}{2}\rangle\langle [f_R]S_RT_R|[2]S_{45}T_{45};\tfrac{1}{2}\tfrac{1}{2}\rangle$$

$$\times(-1)^{S_{12}+S_{45}} \begin{Bmatrix} \frac{1}{2} & T_{12} & T_B \\ \frac{1}{2} & T_{45} & \frac{1}{2} \end{Bmatrix} \begin{Bmatrix} \frac{1}{2} & S_{12} & S_B \\ S_{45} & \frac{1}{2} & S_R \\ \frac{1}{2} & \frac{1}{2} & 1 \end{Bmatrix}, \quad (33)$$

where the ST fractional parentage coefficients $\langle [f_B]S_BT_B|[2]S_{12}T_{12};\frac{1}{2}\frac{1}{2}\rangle$ and $\langle [f_R]S_RT_R|[2]S_{45}T_{45};\frac{1}{2}\frac{1}{2}\rangle$ are the weights of the components with $S_{12} = T_{12}$ and $S_{45} = T_{45}$ in the functions $|[f_B]S_BT_B(r_B)\rangle$ and $|[f_R]S_RT_R(r_R)\rangle$. They can be extracted from the ST parts in Appendix A. For example, $\langle [21]\frac{1}{2}\frac{1}{2}|[2]00;\frac{1}{2}\frac{1}{2}\rangle = \frac{1}{\sqrt{2}}$, $\langle [21]\frac{1}{2}\frac{1}{2}|[2]11;\frac{1}{2}\frac{1}{2}\rangle = -\frac{1}{\sqrt{2}}$, etc.

Thus, finally we have

$$\psi^d_{BR}(\mathbf{r}) = \chi(\mathbf{r})\delta_{B,N}\delta_{R,N} + (-9)^{\frac{1}{3}} \sum_{\substack{m_B m_R \\ \mu_B \mu_R}} C^{J_B M_B}_{L_B m_B S_B \mu_B} C^{J_R M_R}_{L_R m_R S_R \mu_R} \frac{1}{\sqrt{\dim[f_B]}} \frac{1}{\sqrt{\dim[f_R]}} \gamma^X_B \gamma^X_R$$

$$\times \sum_{L,\alpha_k} C^{L,m_B+m_R}_{L_B m_B L_R m_R} A_K I^L_{N_B L_B, N_R L_R}(r;\alpha_k) Y^*_{L,m_B+m_R}(\hat{r})$$

$$\times (-1)^{1/2+S_B+2T_B} \sqrt{2(2T_B+1)(2S_B+1)(2S_R+1)} C^{1M_d}_{S_B\mu_B S_R\mu_R} C^{00}_{T_B t_B T_R t_R}$$

$$\times \sum_{\substack{S_{12}=T_{12}=0,1 \\ S_{45}=T_{45}=0,1}} \langle [f_B] S_B T_B | [2] S_{12} T_{12}; \tfrac{1}{2}\tfrac{1}{2}\rangle \langle [f_R] S_R T_R | [2] S_{45} T_{45}; \tfrac{1}{2}\tfrac{1}{2}\rangle$$

$$\times (-1)^{S_{12}+S_{45}} \begin{Bmatrix} \frac{1}{2} & T_{12} & T_B \\ \frac{1}{2} & T_{45} & \frac{1}{2} \end{Bmatrix} \begin{Bmatrix} \frac{1}{2} & S_{12} & S_B \\ S_{45} & \frac{1}{2} & S_R \\ \frac{1}{2} & \frac{1}{2} & 1 \end{Bmatrix}. \tag{34}$$

In the next sections, we drop the isospin Clebsch-Gordan coefficient $C^{00}_{T_B t_B T_R t_R}$. So all the effective numbers there are meant to be multiplied by the square of this coefficient. For example, $N^d_{\Delta(1232)\Delta(1232)}$ in reality means

$$N^d_{\Delta(1232)\Delta(1232)} = (2.5\text{–}4.3) \times 10^{-2} (C^{00}_{\frac{3}{2}t_B \frac{3}{2}t_R})^2.$$

V. TRANSITIONS $d \to N$-LIKE $+N$-LIKE

Since the pioneering calculation of the baryon spectrum with configuration mixing by Isgur and Karl [22], there were a few works taking into account not only the color-exchange quark-quark potentials, but in addition the chiral-phase–pion-exchange quark-quark interaction [26,27]. In the papers of Obukhovsky and co-workers [4] both π and σ exchanges in chiral-invariant form were included.

All these calculations show that some of the pure harmonic oscillator states (24) correspond to observable excited baryons with a quite good accuracy. Thus, according to Buchmann, Hernandez, and Yazaki [27] for the nucleonlike baryons $J^P, T = \frac{1}{2}^+, \frac{1}{2}$ within $2\hbar\omega$ excitations:

$\lvert\frac{1}{2}^+, \frac{1}{2}\rangle$	α	β	γ	δ	ϵ
$\lvert N(939)\rangle$	$\simeq 0.934\lvert N_0\rangle$	$+0.306\lvert N_1\rangle$	$-0.178\lvert N_2\rangle$	$+0.047\lvert N_3\rangle$	$-0.002\lvert N_4\rangle$
$\lvert N(1440)\rangle$	$\simeq 0.299\lvert N_0\rangle$	$-0.952\lvert N_1\rangle$	$-0.066\lvert N_2\rangle$	$+0.014\lvert N_3\rangle$	$-0.001\lvert N_4\rangle$
$\lvert N(1710)\rangle$	$\simeq 0.193\lvert N_0\rangle$	$-0.009\lvert N_1\rangle$	$+0.977\lvert N_2\rangle$	$-0.084\lvert N_3\rangle$	$+0.016\lvert N_4\rangle$
...					

(35)

We have changed the signs from [27] in accordance with our phase definitions.

In Ref. [4] some of the parameters were chosen to minimize the mixing of $|N_0\rangle$ and $|N_1\rangle$ states in the nucleon wave function. In this case, for the nucleon, $\alpha_N = 0.98$ and $\beta_N = 0.04$ and, for the Roper resonance $N(1440)$, $\alpha_{N(1440)} = 0.12$ and $\beta_{N(1440)} = -0.87$.

Thus, in a first approximation, one can write

$$N(939) \simeq |N_0\rangle,$$
$$N(1440) \simeq |N_1\rangle,$$
$$N(1710) \simeq |N_2\rangle,$$
$$\ldots.$$

In Table I we present the effective numbers for the transitions $d \to |N_i\rangle + |N_j\rangle$. We see that the effective number of the N-N pair in the deuteron is close to 1. That was clear beforehand as far as the nucleon-nucleon pair in the deuteron is dominantly at intermediate and long ranges, including the D-wave component $N^d_{NN} \simeq 1.004$. This number is practically determined by the first term in (25) and (34) [i.e., by the diagram of Fig. 5(a)], $N^d_{NN}(\text{direct}) \simeq 0.996$ and only a little by the interference between the direct and exchange diagrams of Figs. 5(a) and 5(b), $N^d_{NN}(\text{interference}) \simeq 8 \times 10^{-3}$. The contribution of the pure exchange term is very small, $N^d_{NN}(\text{exchange}) \simeq 3.8 \times 10^{-4}$.

All the other numbers in Table I are connected only with the quark-exchange terms in (25) and (34), i.e., with the second diagram of Fig. 5.

We see that the $NN \to NN(1710)$ transition is relatively large, $N^d_{NN(1710)} \simeq N^d_{N_0 N_2} = 2.6 \times 10^{-3}$, and could be measured in the $^2\text{H}(e,e'p)N(1710)$ reaction.

It should be mentioned that the state $|N_4\rangle = |2(01)[1^3]1\tfrac{1}{2}\tfrac{1}{2}\rangle$ is absent in Table I as far as the effective numbers with this state are identically equal to zero [there is no component containing $\varphi_{000}(\mathbf{r}_{12})$ in the $|N_4\rangle$ state].

Let us discuss now the effects of mixing in the baryon wave functions.

First, we should remark that taking into account of an admixture of the $|N_0\rangle$ state in $N(1440), N(1710), \ldots$ leads, when calculating the effective numbers with these baryons, to unphysically large values (see, for example,

the value of $S^d_{NN(1440)} = 2N^d_{NN(1440)}$ in our previous paper [9], where this value was mainly determined by the $|N_0\rangle$ admixture). The reason is as follows. The wave functions of all the excited baryons must be orthogonal to the nucleon's one. But in our six-quark deuteron wave function (4) the nucleons are pure $|N_0\rangle$ states. So taking into account an admixture of the $|N_0\rangle$ state in $N(1440), N(1710), \ldots$, we pick up the pure nucleon-nucleon part of the deuteron (asymptotics and middle range).

The influence of $|N_1\rangle$ and $|N_3\rangle$ admixtures in the $N(1710)$ wave function on the effective numbers $N^d_{NN(1710)}$, $N^d_{N(1440)N(1710)}$, and $N^d_{N(1710)N(1710)}$ is negligible and

$$N^d_{NN(1710)} \simeq N^d_{N_0N_2}, \tag{36}$$

$$N^d_{N(1440)N(1710)} \simeq N^d_{N_1N_2}, \tag{37}$$

$$N^d_{N(1710)N(1710)} \simeq N^d_{N_2N_2}. \tag{38}$$

But due to a small value of $N^d_{N_0N_1} = 8.35 \times 10^{-5}$, the admixture of the $|N_2\rangle$ state in the $N(1440)$ wave function is important for the $N^d_{NN(1440)}$. In this case,

$$N^d_{NN(1440)} \simeq \beta^2_{N(1440)} N^d_{N_0N_1} + \gamma^2_{N(1440)} N^d_{N_0N_2} + 2\beta_{N(1440)}\gamma_{N(1440)} \frac{1}{2J_d+1} \times \sum_{M_B M_R M_d} \int d\mathbf{r}\, \psi^d_{N_0N_1}(\mathbf{r}) \psi^{d^*}_{N_0N_2}(\mathbf{r}). \tag{39}$$

The interference integral is equal to

$$\frac{1}{2J_d+1} \sum_{M_B M_R M_d} \int d\mathbf{r}\, \psi^d_{N_0N_1}(\mathbf{r}) \psi^{d^*}_{N_0N_2}(\mathbf{r}) = 4\sqrt{2} N^d_{N_0N_1} = 4.72 \times 10^{-4}. \tag{40}$$

With the coefficients (35), one gets

$$N^d_{NN(1440)} \simeq 1.5 \times 10^{-4}. \tag{41}$$

However, with the mixing coefficients from Ref. [4],

$$\beta_{N(1440)} = -0.866, \qquad \gamma_{N(1440)} = -0.485, \tag{42}$$

this effective number is

$$N^d_{NN(1440)} \simeq 1.1 \times 10^{-3}. \tag{43}$$

Summarizing, we conclude that a realistic value of the $N^d_{NN(1440)}$ is in the interval

$$N^d_{NN(1440)} = 10^{-4}\text{–}10^{-3} \tag{44}$$

and depends crucially on the admixture of the $|N_2\rangle$ state in the Roper resonance wave function.

VI. TRANSITIONS $D \to$ Δ-LIKE +Δ-LIKE

The amplitudes $\psi^d_{\Delta\text{-like}\,\Delta\text{-like}}$ are of greatest importance. Some of them are quite large as far as they are determined by the large $NN \to \Delta\Delta$ ST-exchange factor,

$$C^{NN\to\Delta\Delta}_{ST=10} = \langle\{([3]_{ST}ST = \tfrac{3}{2}\tfrac{3}{2}) \otimes ([3]_{ST}ST = \tfrac{3}{2}\tfrac{3}{2})\}_{ST=10}|\hat{P}^{ST}_{36}|\{([3]_{ST}ST = \tfrac{1}{2}\tfrac{1}{2}) \otimes ([3]_{ST}ST = \tfrac{1}{2}\tfrac{1}{2})\}_{ST=10}\rangle = \frac{4\sqrt{5}}{27}, \tag{45}$$

compared to the $NN \to NN$ exchange contribution,

$$C^{NN\to NN}_{ST=10} = \langle\{([3]_{ST}ST = \tfrac{1}{2}\tfrac{1}{2}) \otimes ([3]_{ST}ST = \tfrac{1}{2}\tfrac{1}{2})\}_{ST=10}|\hat{P}^{ST}_{36}|\{([3]_{ST}ST = \tfrac{1}{2}\tfrac{1}{2}) \otimes ([3]_{ST}ST = \tfrac{1}{2}\tfrac{1}{2})\}_{ST=10}\rangle = -\tfrac{1}{27}. \tag{46}$$

The most important disintegration amplitudes (25) and (34) are shown in Fig. 7. The corresponding effective numbers are presented in Table II.

In accordance with Buchmann, Hernandez, and Yazaki [27], the $J^P, T = \frac{3}{2}^+, \frac{3}{2}$ baryon wave functions can be presented as

$\lvert\frac{3}{2}^+, \frac{3}{2}\rangle$	α	β	γ	δ
$\lvert\Delta(1232)\rangle$	$\simeq 0.990\lvert\Delta_0\rangle$	$-0.083\lvert\Delta_1\rangle$	$-0.097\lvert\Delta_2\rangle$	$-0.064\lvert\Delta_3\rangle$
$\lvert\Delta(1600)\rangle$	$\simeq 0.069\lvert\Delta_0\rangle$	$+0.991\lvert\Delta_1\rangle$	$-0.102\lvert\Delta_2\rangle$	$-0.057\lvert\Delta_3\rangle$
$\lvert\Delta(1920)\rangle$	$\simeq 0.116\lvert\Delta_0\rangle$	$+0.103\lvert\Delta_1\rangle$	$+0.967\lvert\Delta_2\rangle$	$+0.201\lvert\Delta_3\rangle$
...				

(47)

In contrast, the admixture of the $|\Delta_1\rangle$ component in $|\Delta(1232)\rangle$ is essential in the calculations of Obukhovsky and co-workers [4]:

TABLE I. Effective numbers for the transitions to $|N_i\rangle + |N_j\rangle$. The first line calculated with the microscopical deuteron wave function. The second one calculated with the phenomenological six-quark deuteron wave function (see Sec. II).

$J^P, T = \frac{1}{2}^+, \frac{1}{2}$	0(00)[3] $0\ \frac{1}{2}\ \frac{1}{2}$	2(20)[3] $0\ \frac{1}{2}\ \frac{1}{2}$	2(20)[21] $0\ \frac{1}{2}\ \frac{1}{2}$	2(20)[21] $2\ \frac{3}{2}\ \frac{1}{2}$
0(00)[3] $0\ \frac{1}{2}\ \frac{1}{2}$	0.954 0.946			
2(20)[3] $0\ \frac{1}{2}\ \frac{1}{2}$	8.35×10^{-5} 8.18×10^{-5}	2.92×10^{-5} 2.96×10^{-5}		
2(20)[21] $0\ \frac{1}{2}\ \frac{1}{2}$	2.67×10^{-3} 2.62×10^{-3}	9.33×10^{-4} 9.48×10^{-4}	7.29×10^{-4} 7.41×10^{-4}	
2(20)[21] $2\ \frac{3}{2}\ \frac{1}{2}$	8.92×10^{-6} 9.09×10^{-6}	5.70×10^{-6} 5.44×10^{-6}	4.45×10^{-6} 4.25×10^{-6}	1.24×10^{-6} 1.25×10^{-6}

$$\alpha_\Delta = 0.92 \gg \gamma_\Delta, \delta_\Delta,$$
$$\beta_\Delta = -0.35. \tag{48}$$

In this latter case, the mixing of the first and second components of the expression (47) in the $\Delta(1232)$ wave function is important and must be taken into account when calculating the effective number $N^d_{\Delta\Delta}$. One has

$$N^d_{\Delta(1232)\Delta(1232)} \simeq \alpha^4_\Delta N^d_{\Delta_0\Delta_0} + \beta^4_\Delta N^d_{\Delta_1\Delta_1} + 4\alpha^2_\Delta\beta^2_\Delta N^d_{\Delta_0\Delta_1} + 2\alpha^2_\Delta\beta^2_\Delta \frac{1}{2J_d+1}\sum_{M_B M_R M_d}\int d\mathbf{r}\,\psi^d_{\Delta_0\Delta_0}(\mathbf{r})\psi^{d^*}_{\Delta_1\Delta_1}(\mathbf{r})$$
$$+4\alpha^3_\Delta\beta_\Delta \frac{1}{2J_d+1}\sum_{M_B M_R M_d}\int d\mathbf{r}\,\psi^d_{\Delta_0\Delta_0}(\mathbf{r})\psi^{d^*}_{\Delta_0\Delta_1}(\mathbf{r})$$
$$+4\alpha_\Delta\beta^3_\Delta \frac{1}{2J_d+1}\sum_{M_B M_R M_d}\int d\mathbf{r}\,\psi^d_{\Delta_1\Delta_1}(\mathbf{r})\psi^{d^*}_{\Delta_0\Delta_1}(\mathbf{r}). \tag{49}$$

The interference integrals are equal to

$$\frac{1}{2J_d+1}\sum_{M_B M_R M_d}\int d\mathbf{r}\,\psi^d_{\Delta_0\Delta_0}(\mathbf{r})\psi^{d^*}_{\Delta_1\Delta_1}(\mathbf{r}) = 8.37\times10^{-3}, \tag{50}$$

$$\frac{1}{2J_d+1}\sum_{M_B M_R M_d}\int d\mathbf{r}\,\psi^d_{\Delta_0\Delta_0}(\mathbf{r})\psi^{d^*}_{\Delta_0\Delta_1}(\mathbf{r}) = -1.42\times10^{-2}, \tag{51}$$

$$\frac{1}{2J_d+1}\sum_{M_B M_R M_d}\int d\mathbf{r}\,\psi^d_{\Delta_1\Delta_1}(\mathbf{r})\psi^{d^*}_{\Delta_0\Delta_1}(\mathbf{r}) = -3.94\times10^{-3}. \tag{52}$$

So if we put the numbers (48) into the expression (49), we get

$$N^d_{\Delta(1232)\Delta(1232)} = 4.24\times10^{-2}. \tag{53}$$

But if we put the mixing coefficients (47), we get

$$N^d_{\Delta(1232)\Delta(1232)} = 3.39\times10^{-2}. \tag{54}$$

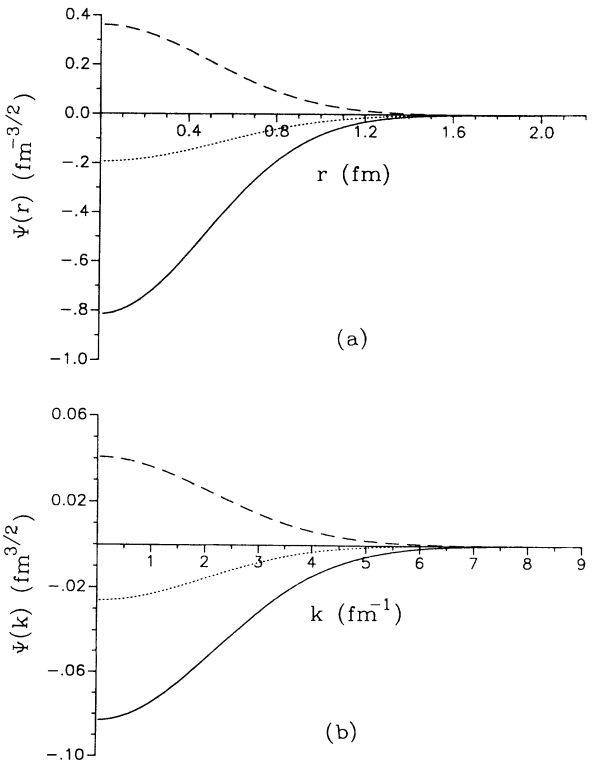

FIG. 7. (a) $\psi^d_{\Delta_0\Delta_0}(r)$ (solid line), $\psi^d_{\Delta_0\Delta_1}(r)$ (dashed line), and $\psi^d_{\Delta_1\Delta_1}(r)$ (dotted line) in the coordinate representation; (b) the same in the momentum representation.

We see that taking into account the mixing in the $\Delta(1232)$ wave function increases $N^d_{\Delta\Delta}$ from 3.04×10^{-2} up to 3.4×10^{-2}–4.24×10^{-2}. Bearing in mind some uncertainty in the six-quark deuteron wave function, we can conclude that the realistic value is in the interval

$$N^d_{\Delta(1232)\Delta(1232)} = (2.5\text{–}4.3)\times10^{-2}. \tag{55}$$

We have mentioned earlier that the quark-exchange transitions are essential only in the s wave of the relative motion. Here the quark-exchange contribution to $NN \to \Delta\Delta$ exceeds the meson-exchange contribution approximately one order of magnitude [10]. In the standard meson-exchange coupled-channels calculations [12], the $\Delta\Delta$ probability in the $^3S_1$ wave in the deuteron is less than 0.1% and full probability ($^3S_1 + ^3D_1 + ^7D_1 + ^7G_1$) is less than 1%.

We see that in any case the quark-exchange $NN \to \Delta\Delta$ transition is essentially larger (at least 3 times) than the usual meson-exchange $\Delta\Delta$ component in the deuteron. So in a process with Δ as a spectator, such as $^2\mathrm{H}(e,e'p)\Delta$, we shall see the quark exchange currents, i.e., the six-quark structure of the deuteron.

The mixing of the different states (47) is of some importance for the $N^d_{\Delta(1232)\Delta(1600)}$ and $N^d_{\Delta(1600)\Delta(1600)}$.

Expressions similar to (49) lead to

$$N^d_{\Delta(1232)\Delta(1600)} \simeq 5.8\times10^{-3}, \tag{56}$$

$$N^d_{\Delta(1600)\Delta(1600)} \simeq 1.4\times10^{-3}. \tag{57}$$

The mixing is of crucial importance for the effective numbers with higher resonances. These effective numbers are entirely determined by the small admixtures of $|\Delta_0\rangle$ and $|\Delta_1\rangle$ states. The reason is that the $N^d_{\Delta_0\Delta_0}$, $N^d_{\Delta_0\Delta_1}$, and $N^d_{\Delta_1\Delta_1}$ and the interference terms (50)–(52) are two or three orders larger than $N^d_{\Delta_0\Delta_2}, N^d_{\Delta_0\Delta_3}, N^d_{\Delta_1\Delta_2}, \ldots$. For instance, taking into account the admixtures of $|\Delta_0\rangle$ and $|\Delta_1\rangle$ in $|\Delta(1920)\rangle$ instead of $N^d_{\Delta(1232)\Delta(1920)} \simeq N^d_{\Delta_0\Delta_2}$, one has

$$N^d_{\Delta(1232)\Delta(1920)} \simeq 3.2\times10^{-4}. \tag{58}$$

VII. TRANSITIONS $d \to N$-LIKE + $N^{(-)}$-LIKE AND $d \to N^{(-)}$-LIKE + $N^{(-)}$-LIKE

All the effective numbers $N^d_{N_i N_j^{(-)}}$ and $N^d_{N_i^{(-)} N_j^{(-)}}$ for the baryons $J^P, T = \frac{1}{2}^-, \frac{1}{2}$ and $\frac{3}{2}^-, \frac{1}{2}$ are shown in Tables III–VII. In these tables the states

$$|3(11)[21]1\tfrac{1}{2}\tfrac{1}{2}\rangle,$$
$$|3(11)[21]1\tfrac{3}{2}\tfrac{1}{2}\rangle,$$
$$|3(11)[21]2\tfrac{3}{2}\tfrac{1}{2}\rangle,$$
$$|3(11)[21]2\tfrac{1}{2}\tfrac{1}{2}\rangle,$$
$$|3(30)[111]1\tfrac{1}{2}\tfrac{1}{2}\rangle$$

are absent as far as the corresponding effective numbers are identically equal to zero [there is no component containing $\varphi_{000}(\mathbf{r}_{12})$ in all these states].

The only possible state with $L=3$ $|3(30)[21]3\frac{3}{2}\frac{1}{2}\rangle$ is also absent in Tables III–VII containing particles $J^P, T = \frac{3}{2}^-, \frac{1}{2}$. First, its admixture in the low-lying resonances is small, and second, the corresponding effective numbers are small, too. In the first approximation,

$$N(1535) \simeq |1(10)[21]1\tfrac{1}{2}\tfrac{1}{2} : \tfrac{1}{2}\rangle,$$
$$N(1650) \simeq |1(10)[21]1\tfrac{3}{2}\tfrac{1}{2} : \tfrac{1}{2}\rangle,$$
$$\ldots,$$
$$N(1520) \simeq |1(10)[21]1\tfrac{1}{2}\tfrac{1}{2} : \tfrac{3}{2}\rangle,$$
$$N(1700) \simeq |1(10)[21]1\tfrac{3}{2}\tfrac{1}{2} : \tfrac{3}{2}\rangle,$$
$$\ldots.$$

From Tables III–VII one can conclude that the transitions

$$d \to N(1520) + N(1520),$$
$$d \to N(1520) + N(1535),$$
$$d \to N + N(1520),$$
$$d \to N(1535) + N(1700),$$
$$d \to N(1520) + N(1700),$$
$$d \to N(1535) + N(1650)$$

are of great importance and the corresponding effective numbers are $(1\text{–}3)\times10^{-3}$. In addition, we should mention the transitions

TABLE II. Effective numbers for the transitions to $|\Delta_i\rangle + |\Delta_j\rangle$. The first line calculated with the microscopical deuteron wave function. The second one calculated with the phenomenological six-quark deuteron wave function (see Sec. II).

$J^P, T = \frac{3}{2}^+ \frac{3}{2}$ / $J^P, T = \frac{3}{2}^+, \frac{3}{2}$	0(00)[3] $0\ \frac{3}{2}\ \frac{3}{2}$	2(20)[3] $0\ \frac{3}{2}\ \frac{3}{2}$	2(20)[3] $2\ \frac{3}{2}\ \frac{3}{2}$	2(20)[21] $2\ \frac{1}{2}\ \frac{3}{2}$
0(00)[3] $0\ \frac{3}{2}\ \frac{3}{2}$	3.04×10^{-2} 2.12×10^{-2}			
2(20)[3] $0\ \frac{3}{2}\ \frac{3}{2}$	6.68×10^{-3} 6.54×10^{-3}	2.33×10^{-3} 2.37×10^{-3}		
2(20)[3] $2\ \frac{3}{2}\ \frac{3}{2}$	4.46×10^{-5} 4.55×10^{-5}	2.85×10^{-4} 2.72×10^{-4}	2.28×10^{-5} 2.27×10^{-5}	
2(20)[21] $2\ \frac{1}{2}\ \frac{3}{2}$	8.92×10^{-6} 9.09×10^{-6}	5.70×10^{-6} 5.44×10^{-6}	3.08×10^{-5} 3.13×10^{-5}	2.49×10^{-5} 2.52×10^{-5}

TABLE III. Effective numbers for the transitions to N-like + $N^{(-)}$-like ($J = \frac{1}{2}$). The first line calculated with the microscopical deuteron wave function. The second one calculated with the phenomenological six-quark deuteron wave function (see Sec. II).

$J^P, T = \frac{1}{2}^-, \frac{1}{2}$	$J^P, T = \frac{1}{2}^+, \frac{1}{2}$ 0(00)[3] $0\ \frac{1}{2}\ \frac{1}{2}$	2(20)[3] $0\ \frac{1}{2}\ \frac{1}{2}$	2(20)[21] $0\ \frac{1}{2}\ \frac{1}{2}$	2(20)[21] $2\ \frac{3}{2}\ \frac{1}{2}$
1(10)[21]	8.76×10^{-4}	3.01×10^{-4}	2.36×10^{-4}	4.71×10^{-5}
$1\ \frac{1}{2}\ \frac{1}{2}$	8.57×10^{-4}	3.07×10^{-4}	2.40×10^{-4}	4.80×10^{-5}
1(10)[21]	4.38×10^{-4}	1.51×10^{-4}	1.18×10^{-4}	2.83×10^{-6}
$1\ \frac{3}{2}\ \frac{1}{2}$	4.29×10^{-4}	1.54×10^{-4}	1.20×10^{-4}	2.88×10^{-6}
3(30)[3]	2.83×10^{-6}	1.82×10^{-6}	5.83×10^{-5}	1.17×10^{-5}
$1\ \frac{1}{2}\ \frac{1}{2}$	2.88×10^{-6}	1.74×10^{-6}	5.57×10^{-5}	1.11×10^{-5}
3(30)[21]	2.71×10^{-4}	1.75×10^{-4}	1.37×10^{-4}	2.73×10^{-5}
$1\ \frac{1}{2}\ \frac{1}{2}$	2.76×10^{-4}	1.67×10^{-4}	1.31×10^{-4}	2.61×10^{-5}
3(30)[21]	1.36×10^{-4}	8.75×10^{-5}	6.83×10^{-5}	1.64×10^{-6}
$1\ \frac{3}{2}\ \frac{1}{2}$	1.38×10^{-4}	8.35×10^{-5}	6.52×10^{-5}	1.57×10^{-6}

TABLE IV. Effective numbers for the transitions to N-like + $N^{(-)}$-like ($J = \frac{3}{2}$). The first line calculated with the microscopical deuteron wave function. The second one calculated with the phenomenological six-quark deuteron wave function (see Sec. II).

$J^P, T = \frac{3}{2}^-, \frac{1}{2}$	$J^P, T = \frac{1}{2}^+, \frac{1}{2}$ 0(00)[3] $0\ \frac{1}{2}\ \frac{1}{2}$	2(20)[3] $0\ \frac{1}{2}\ \frac{1}{2}$	2(20)[21] $0\ \frac{1}{2}\ \frac{1}{2}$	2(20)[21] $2\ \frac{3}{2}\ \frac{1}{2}$
1(10)[21]	1.75×10^{-3}	6.03×10^{-4}	4.71×10^{-4}	1.06×10^{-5}
$1\ \frac{1}{2}\ \frac{1}{2}$	1.71×10^{-3}	6.14×10^{-4}	4.80×10^{-4}	1.07×10^{-5}
1(10)[21]	8.76×10^{-4}	3.01×10^{-4}	2.36×10^{-4}	2.62×10^{-6}
$1\ \frac{3}{2}\ \frac{1}{2}$	8.57×10^{-4}	3.07×10^{-4}	2.40×10^{-4}	2.67×10^{-6}
3(30)[3]	5.65×10^{-6}	3.64×10^{-6}	1.17×10^{-4}	2.80×10^{-6}
$1\ \frac{1}{2}\ \frac{1}{2}$	5.76×10^{-6}	3.48×10^{-6}	1.11×10^{-4}	2.67×10^{-6}
3(30)[21]	5.43×10^{-4}	3.50×10^{-4}	2.73×10^{-4}	6.56×10^{-6}
$1\ \frac{1}{2}\ \frac{1}{2}$	5.53×10^{-4}	3.34×10^{-4}	2.61×10^{-4}	6.26×10^{-6}
3(30)[21]	2.71×10^{-4}	1.75×10^{-4}	1.37×10^{-4}	1.53×10^{-6}
$1\ \frac{3}{2}\ \frac{1}{2}$	2.76×10^{-4}	1.67×10^{-4}	1.31×10^{-4}	1.46×10^{-6}

TABLE V. Effective numbers for the transitions to $N^{(-)}$-like ($J = \frac{1}{2}$) + $N^{(-)}$-like ($J = \frac{1}{2}$). The first line calculated with the microscopical deuteron wave function. The second one calculated with the phenomenological six-quark deuteron wave function (see Sec. II).

$J^P, T = \frac{1}{2}^-, \frac{1}{2}$	$J^P, T = \frac{1}{2}^-, \frac{1}{2}$ 1(10)[21] $1\ \frac{1}{2}\ \frac{1}{2}$	1(10)[21] $1\ \frac{3}{2}\ \frac{1}{2}$	3(30)[3] $1\ \frac{1}{2}\ \frac{1}{2}$	3(30)[21] $1\ \frac{1}{2}\ \frac{1}{2}$	3(30)[21] $1\ \frac{3}{2}\ \frac{1}{2}$
1(10)[21]	3.51×10^{-4}				
$1\ \frac{1}{2}\ \frac{1}{2}$	3.45×10^{-4}				
1(10)[21]	1.23×10^{-3}	7.74×10^{-5}			
$1\ \frac{3}{2}\ \frac{1}{2}$	1.21×10^{-3}	7.58×10^{-5}			
3(30)[3]	5.16×10^{-5}	1.67×10^{-4}	2.56×10^{-7}		
$1\ \frac{1}{2}\ \frac{1}{2}$	5.18×10^{-5}	1.69×10^{-4}	2.44×10^{-7}		
3(30)[21]	1.21×10^{-4}	3.90×10^{-4}	2.46×10^{-5}	5.76×10^{-5}	
$1\ \frac{1}{2}\ \frac{1}{2}$	1.21×10^{-4}	3.96×10^{-4}	2.35×10^{-5}	5.50×10^{-5}	
3(30)[21]	3.90×10^{-4}	2.44×10^{-5}	9.82×10^{-5}	2.30×10^{-4}	1.44×10^{-5}
$1\ \frac{3}{2}\ \frac{1}{2}$	3.96×10^{-4}	2.48×10^{-5}	9.38×10^{-5}	2.20×10^{-4}	1.37×10^{-5}

TABLE VI. Effective numbers for the transitions to $N^{(-)}$-like ($J=\frac{3}{2}$) + $N^{(-)}$-like ($J=\frac{3}{2}$). The first line calculated with the microscopical deuteron wave function. The second one calculated with the phenomenological six-quark deuteron wave function (see Sec. II).

$J^P,T=\frac{3}{2}^-,\frac{1}{2}$ / $J^P,T=\frac{3}{2}^-,\frac{1}{2}$	1(10)[21] $1\ \frac{1}{2}\ \frac{1}{2}$	1(10)[21] $1\ \frac{3}{2}\ \frac{1}{2}$	3(30)[3] $1\ \frac{1}{2}\ \frac{1}{2}$	3(30)[21] $1\ \frac{1}{2}\ \frac{1}{2}$	3(30)[21] $1\ \frac{3}{2}\ \frac{1}{2}$
1(10)[21] $1\ \frac{1}{2}\ \frac{1}{2}$	3.23×10^{-3} 3.17×10^{-3}				
1(10)[21] $1\ \frac{3}{2}\ \frac{1}{2}$	1.31×10^{-3} 1.29×10^{-3}	1.53×10^{-4} 1.49×10^{-4}			
3(30)[3] $1\ \frac{1}{2}\ \frac{1}{2}$	4.48×10^{-4} 4.53×10^{-4}	1.84×10^{-4} 1.86×10^{-4}	2.56×10^{-6} 2.44×10^{-6}		
3(30)[21] $1\ \frac{1}{2}\ \frac{1}{2}$	1.05×10^{-3} 1.06×10^{-3}	4.30×10^{-4} 4.35×10^{-4}	2.46×10^{-4} 2.34×10^{-4}	5.76×10^{-4} 5.49×10^{-4}	
3(30)[21] $1\ \frac{3}{2}\ \frac{1}{2}$	4.30×10^{-4} 4.35×10^{-4}	4.86×10^{-5} 4.93×10^{-5}	9.82×10^{-5} 9.38×10^{-5}	2.30×10^{-4} 2.20×10^{-4}	2.79×10^{-5} 2.66×10^{-5}

$$d \to N + N(1535),$$
$$d \to N + N(1700),$$

and

$$d \to N(1520) + |3(30)[21]1\tfrac{1}{2}\tfrac{1}{2} : \tfrac{3}{2}\rangle,$$
$$d \to N(1535) + |3(30)[21]1\tfrac{1}{2}\tfrac{1}{2} : \tfrac{3}{2}\rangle,$$
$$d \to N(1520) + |3(30)[21]1\tfrac{1}{2}\tfrac{1}{2} : \tfrac{1}{2}\rangle,$$

which are of magnitude $(8\text{–}10)\times10^{-4}$.

Let us now discuss the effects of possible mixing in the baryons $N(1535)$, $N(1650)$, $N(1520)$, and $N(1700)$ on the corresponding effective numbers. It is well seen from the tables that only the mixture of $|N_1^{(-)}\rangle$ and $|N_2^{(-)}\rangle$ states in these baryons is of some importance.

Unfortunately, there are no detailed calculations of the configuration mixing in the negative parity baryons with the Hamiltonian including both the color-, π-, and σ-exchange potentials on the quark level. So we restrict ourselves to the configuration mixing calculated with only the color-exchange potentials by Kalman and Tran [28]. One should mention that this paper reports a small mixing of the $|N_1^{(-)}\rangle$ and $|N_2^{(-)}\rangle$ states in the low-lying baryons $J^P,T=\frac{1}{2}^-,\frac{1}{2}$ $N(1535)$ and $N(1650)$:

$$\begin{aligned} |N(1535)\rangle &= -0.8996|N_1^{(-)}\rangle \\ &\quad +0.0366|N_2^{(-)}\rangle + \cdots, \\ |N(1650)\rangle &= -0.0080|N_1^{(-)}\rangle \\ &\quad +0.9849|N_2^{(-)}\rangle + \cdots, \end{aligned} \tag{59}$$

in contrast with the result of Isgur and Karl [22] where the mixing coefficients are 0.85 and 0.53 for the $|N(1535)\rangle$ and 0.53 and -0.85 for the $|N(1650)\rangle$. But in the Isgur-Karl paper [22], only the first-order perturbations in the anharmonicity and in the hyperfine interaction was taken into account and only the $|N_1^{(-)}\rangle$ and $|N_2^{(-)}\rangle$ states were used as a basis, while all $N=1$ and $N=3$ states were used in Ref. [28].

For the $J^P,T=\frac{3}{2}^-,\frac{1}{2}$ low-lying baryons, Kalman and Tran report

$$\begin{aligned} |N(1520)\rangle &= -0.8977|N_1^{(-)}\rangle \\ &\quad +0.0637|N_2^{(-)}\rangle + \cdots, \end{aligned} \tag{60}$$

$$\begin{aligned} |N(1700)\rangle &= -0.0590|N_1^{(-)}\rangle \\ &\quad -0.9809|N_2^{(-)}\rangle + \cdots. \end{aligned} \tag{61}$$

TABLE VII. Effective numbers for the transitions to $N^{(-)}$-like ($J=\frac{1}{2}$) + $N^{(-)}$-like ($J=\frac{3}{2}$). The first line calculated with the microscopical deuteron wave function. The second one calculated with the phenomenological six-quark deuteron wave function (see Sec. II).

$J^P,T=\frac{1}{2}^-,\frac{1}{2}$ / $J^P,T=\frac{3}{2}^-,\frac{1}{2}$	1(10)[21] $1\ \frac{1}{2}\ \frac{1}{2}$	1(10)[21] $1\ \frac{3}{2}\ \frac{1}{2}$	3(30)[3] $1\ \frac{1}{2}\ \frac{1}{2}$	3(30)[21] $1\ \frac{1}{2}\ \frac{1}{2}$	3(30)[21] $1\ \frac{3}{2}\ \frac{1}{2}$
1(10)[21] $1\ \frac{1}{2}\ \frac{1}{2}$	2.53×10^{-3} 2.48×10^{-3}	1.99×10^{-4} 1.96×10^{-4}	3.44×10^{-4} 3.49×10^{-4}	8.07×10^{-4} 8.18×10^{-4}	7.38×10^{-5} 7.35×10^{-5}
1(10)[21] $1\ \frac{3}{2}\ \frac{1}{2}$	1.57×10^{-3} 1.54×10^{-3}	6.28×10^{-5} 6.15×10^{-5}	2.12×10^{-4} 2.16×10^{-4}	4.98×10^{-4} 5.05×10^{-4}	2.00×10^{-5} 2.03×10^{-5}
3(30)[3] $1\ \frac{1}{2}\ \frac{1}{2}$	3.44×10^{-4} 3.49×10^{-4}	3.15×10^{-5} 3.14×10^{-5}	2.05×10^{-6} 1.95×10^{-6}	1.96×10^{-4} 1.88×10^{-4}	1.23×10^{-5} 1.17×10^{-5}
3(30)[21] $1\ \frac{1}{2}\ \frac{1}{2}$	8.07×10^{-4} 8.18×10^{-4}	7.38×10^{-5} 7.35×10^{-5}	1.96×10^{-4} 1.88×10^{-4}	4.60×10^{-4} 4.40×10^{-4}	2.88×10^{-5} 2.75×10^{-5}
3(30)[21] $1\ \frac{3}{2}\ \frac{1}{2}$	4.98×10^{-4} 5.05×10^{-4}	2.00×10^{-5} 2.03×10^{-5}	1.23×10^{-4} 1.17×10^{-4}	2.88×10^{-4} 2.75×10^{-4}	1.15×10^{-5} 1.10×10^{-5}

To estimate the effect of mixing, we need interference terms in addition to Tables III–VII:

$$\frac{1}{2J_d+1}\sum_{M_B M_R M_d}\int d\mathbf{r}\,\psi^d_{N_0 N_1^{(-)}(J=\frac{1}{2})}(\mathbf{r})\psi^{d^*}_{N_0 N_2^{(-)}(J=\frac{1}{2})}(\mathbf{r})=0, \tag{62}$$

$$\frac{1}{2J_d+1}\sum_{M_B M_R M_d}\int d\mathbf{r}\,\psi^d_{N_0 N_1^{(-)}(J=\frac{3}{2})}(\mathbf{r})\psi^{d^*}_{N_0 N_2^{(-)}(J=\frac{3}{2})}(\mathbf{r})=0, \tag{63}$$

$$\frac{1}{2J_d+1}\sum_{M_B M_R M_d}\int d\mathbf{r}\,\psi^d_{N_1^{(-)}(J=\frac{1}{2})N_1^{(-)}(J=\frac{1}{2})}(\mathbf{r})\psi^{d^*}_{N_1^{(-)}(J=\frac{1}{2})N_2^{(-)}(J=\frac{1}{2})}(\mathbf{r})\simeq 6.1\times 10^{-4}, \tag{64}$$

$$\frac{1}{2J_d+1}\sum_{M_B M_R M_d}\int d\mathbf{r}\,\psi^d_{N_1^{(-)}(J=\frac{3}{2})N_1^{(-)}(J=\frac{3}{2})}(\mathbf{r})\psi^{d^*}_{N_1^{(-)}(J=\frac{3}{2})N_2^{(-)}(J=\frac{3}{2})}(\mathbf{r})\simeq -2\times 10^{-3}, \tag{65}$$

$$\frac{1}{2J_d+1}\sum_{M_B M_R M_d}\int d\mathbf{r}\,\psi^d_{N_1^{(-)}(J=\frac{1}{2})N_1^{(-)}(J=\frac{3}{2})}(\mathbf{r})\psi^{d^*}_{N_1^{(-)}(J=\frac{1}{2})N_2^{(-)}(J=\frac{3}{2})}(\mathbf{r})\simeq 2\times 10^{-3}. \tag{66}$$

One should mention that it is easy to calculate the necessary effective numbers with arbitrary mixing coefficients using Tables III–VII and the interference terms (62)–(66). But now we shall use the coefficients (59)–(61). One has

$$\begin{aligned}
&N^d_{N(1520)N(1520)}\simeq 2.4\times 10^{-3},\\
&N^d_{N(1520)N(1535)}\simeq 1.6\times 10^{-3},\\
&N^d_{NN(1520)}\simeq 1.4\times 10^{-3},\\
&N^d_{N(1535)N(1700)}\simeq 1.3\times 10^{-3},\\
&N^d_{N(1535)N(1650)}\simeq 9.6\times 10^{-4},\\
&N^d_{N(1520)N(1700)}\simeq 8.4\times 10^{-4},\\
&N^d_{NN(1700)}\simeq 8.6\times 10^{-4},\\
&N^d_{NN(1535)}\simeq 7.1\times 10^{-4},\\
&\cdots.
\end{aligned} \tag{67}$$

VIII. CONCLUSION

In this paper we have calculated a great number of the virtual $d\to$baryon+baryon quark-exchange amplitudes and the corresponding effective numbers. In combination with our previous papers [9,10], these numbers are the basis for a systematical study of the deuteron six-quark structure in $^2\mathrm{H}(e,e'p)\Delta$ and $^2\mathrm{H}(e,e'p)N^*$ processes. The amplitudes mentioned above could be a basis not only for these reactions, but also for the other ones with one of the excited baryons as a spectator or in more complicated situations.

Why is the study of the reactions of such type important? The achievement of the constituent quark concepts[3] in the simplest nuclear system, NN, is mainly in explanation of the soft-core-like behavior of this system at small distances, nucleon-nucleon phase shifts, deuteron properties, etc. (see Introduction). This achievement is very essential. But, nevertheless, any serious concept must not only explain existing phenomena, but also predict new ones. The quark-exchange process which originates from the Pauli principle on the constituent quark level is such a phenomenon. And one of the tasks is, in our opinion, to try to observe them.

[3]For physics which could be responsible for constituent quark structure of baryons, see [18,19].

ACKNOWLEDGMENTS

One of the authors (L.Ya.G.) thanks the Alexander von Humboldt Foundation for financial support and the Institute of Theoretical Physics at the University of Tuebingen for their hospitality and good working conditions. The discussions with Prof. A. Faessler, Prof. V. G. Neudatchin, Prof. I. T. Obukhovsky, and Prof. E. W. Schmid are gratefully acknowledged. He is also most grateful to Dr. A. Buchmann and Dr. E. Hernandez for the mixing coefficients in the baryon wave functions.

APPENDIX A

In this appendix we show the spatial and spin-isospin parts of the wave functions for baryons $J^P,T=\frac{1}{2}^+,\frac{1}{2}$; $\frac{1}{2}^-,\frac{1}{2}$; $\frac{3}{2}^-,\frac{1}{2}$; $\frac{3}{2}^+,\frac{3}{2}$ within the bands $N=0,1,2$. The wave functions are constructed in correspondence with the expression (23).

1. Spatial parts $|N(\lambda\mu)[f]L(r)\rangle$

The choice of Jacobi coordinates is

$$\begin{aligned}
\mathbf{r}_{12}&=\frac{\mathbf{r}_1-\mathbf{r}_2}{\sqrt{2}},\\
\mathbf{r}_{45}&=\frac{\mathbf{r}_4-\mathbf{r}_5}{\sqrt{2}},\\
\boldsymbol{\rho}&=\frac{\mathbf{r}_1+\mathbf{r}_2-2\mathbf{r}_3}{\sqrt{6}},\\
\boldsymbol{\eta}&=\frac{\mathbf{r}_4+\mathbf{r}_5-2\mathbf{r}_6}{\sqrt{6}}.
\end{aligned}$$

a. $N=0$

$$|0(00)[3]0(111)\rangle=\varphi_{000}(\mathbf{r}_{12})\varphi_{000}(\boldsymbol{\rho}).$$

b. $N=1$

$$\begin{aligned}
|1(10)[21]1(112)\rangle&=\varphi_{000}(\mathbf{r}_{12})\varphi_{11M}(\boldsymbol{\rho}),\\
|1(10)[21]1(121)\rangle&=\varphi_{11M}(\mathbf{r}_{12})\varphi_{000}(\boldsymbol{\rho}).
\end{aligned}$$

c. $N = 2$

$$|2(20)[3]0(111)\rangle = \frac{1}{\sqrt{2}}\varphi_{200}(\mathbf{r}_{12})\varphi_{000}(\boldsymbol{\rho}) + \frac{1}{\sqrt{2}}\varphi_{000}(\mathbf{r}_{12})\varphi_{200}(\boldsymbol{\rho}),$$

$$|2(20)[3]2(111)\rangle = \frac{1}{\sqrt{2}}\varphi_{22M}(\mathbf{r}_{12})\varphi_{000}(\boldsymbol{\rho}) + \frac{1}{\sqrt{2}}\varphi_{000}(\mathbf{r}_{12})\varphi_{22M}(\boldsymbol{\rho}),$$

$$|2(20)[21]0(112)\rangle = \frac{1}{\sqrt{2}}\varphi_{000}(\mathbf{r}_{12})\varphi_{200}(\boldsymbol{\rho}) - \frac{1}{\sqrt{2}}\varphi_{200}(\mathbf{r}_{12})\varphi_{000}(\boldsymbol{\rho}),$$

$$|2(20)[21]0(121)\rangle = -\sum_{m_1,m_2} C^{00}_{1m_1 1m_2}\varphi_{11m_1}(\mathbf{r}_{12})\varphi_{11m_2}(\boldsymbol{\rho}),$$

$$|2(20)[21]2(112)\rangle = \frac{1}{\sqrt{2}}\varphi_{000}(\mathbf{r}_{12})\varphi_{22M}(\boldsymbol{\rho}) - \frac{1}{\sqrt{2}}\varphi_{22M}(\mathbf{r}_{12})\varphi_{000}(\boldsymbol{\rho}),$$

$$|2(20)[21]2(121)\rangle = -\sum_{m_1,m_2} C^{2M}_{1m_1 1m_2}\varphi_{11m_1}(\mathbf{r}_{12})\varphi_{11m_2}(\boldsymbol{\rho}),$$

$$|2(01)[1^3]1(123)\rangle = \sum_{m_1,m_2} C^{1M}_{1m_1 1m_2}\varphi_{11m_1}(\mathbf{r}_{12})\varphi_{11m_2}(\boldsymbol{\rho}).$$

2. ST parts: $|[f]ST(r)\rangle$

$$|[3]\tfrac{1}{2}\tfrac{1}{2}(111)\rangle = \frac{1}{\sqrt{2}}|(S_{12}=0)S=\tfrac{1}{2}\rangle|(T_{12}=0)T=\tfrac{1}{2}\rangle + \frac{1}{\sqrt{2}}|(S_{12}=1)S=\tfrac{1}{2}\rangle|(T_{12}=1)T=\tfrac{1}{2}\rangle,$$

$$|[3]\tfrac{3}{2}\tfrac{3}{2}(111)\rangle = |(S_{12}=1)S=\tfrac{3}{2}\rangle|(T_{12}=1)T=\tfrac{3}{2}\rangle,$$

$$|[21]\tfrac{1}{2}\tfrac{1}{2}(112)\rangle = \frac{1}{\sqrt{2}}|(S_{12}=0)S=\tfrac{1}{2}\rangle|(T_{12}=0)T=\tfrac{1}{2}\rangle - \frac{1}{\sqrt{2}}|(S_{12}=1)S=\tfrac{1}{2}\rangle|(T_{12}=1)T=\tfrac{1}{2}\rangle,$$

$$|[21]\tfrac{1}{2}\tfrac{1}{2}(121)\rangle = \frac{1}{\sqrt{2}}|(S_{12}=0)S=\tfrac{1}{2}\rangle|(T_{12}=1)T=\tfrac{1}{2}\rangle + \frac{1}{\sqrt{2}}|(S_{12}=1)S=\tfrac{1}{2}\rangle|(T_{12}=0)T=\tfrac{1}{2}\rangle,$$

$$|[21]\tfrac{1}{2}\tfrac{3}{2}(112)\rangle = |(S_{12}=1)S=\tfrac{1}{2}\rangle|(T_{12}=1)T=\tfrac{3}{2}\rangle,$$

$$|[21]\tfrac{1}{2}\tfrac{3}{2}(121)\rangle = |(S_{12}=0)S=\tfrac{1}{2}\rangle|(T_{12}=1)T=\tfrac{3}{2}\rangle,$$

$$|[21]\tfrac{3}{2}\tfrac{1}{2}(112)\rangle = |(S_{12}=1)S=\tfrac{3}{2}\rangle|(T_{12}=1)T=\tfrac{1}{2}\rangle,$$

$$|[21]\tfrac{3}{2}\tfrac{1}{2}(121)\rangle = |(S_{12}=1)S=\tfrac{3}{2}\rangle|(T_{12}=0)T=\tfrac{1}{2}\rangle,$$

$$|[1^3]\tfrac{1}{2}\tfrac{1}{2}(123)\rangle = \frac{1}{\sqrt{2}}|(S_{12}=1)S=\tfrac{1}{2}\rangle|(T_{12}=0)T=\tfrac{1}{2}\rangle - \frac{1}{\sqrt{2}}|(S_{12}=0)S=\tfrac{1}{2}\rangle|(T_{12}=1)T=\tfrac{1}{2}\rangle,$$

where

$$|(S_{12}=0)S=\tfrac{1}{2}\rangle = \sum_{m_1,m_2,m_3} C^{\frac{1}{2}M_S}_{00\frac{1}{2}m_3} C^{00}_{\frac{1}{2}m_1\frac{1}{2}m_2}|\tfrac{1}{2}m_1\rangle|\tfrac{1}{2}m_2\rangle|\tfrac{1}{2}m_3\rangle,$$

$$|(S_{12}=1)S=\tfrac{1}{2}\rangle = \sum_{m_1,m_2,m_3,m_{12}} C^{\frac{1}{2}M_S}_{1m_{12}\frac{1}{2}m_3} C^{1m_{12}}_{\frac{1}{2}m_1\frac{1}{2}m_2}|\tfrac{1}{2}m_1\rangle|\tfrac{1}{2}m_2\rangle|\tfrac{1}{2}m_3\rangle,$$

$$|(S_{12}=1)S=\tfrac{3}{2}\rangle = \sum_{m_1,m_2,m_3,m_{12}} C^{\frac{3}{2}M_S}_{1m_{12}\frac{1}{2}m_3} C^{1m_{12}}_{\frac{1}{2}m_1\frac{1}{2}m_2}|\tfrac{1}{2}m_1\rangle|\tfrac{1}{2}m_2\rangle|\tfrac{1}{2}m_3\rangle.$$

The same for $|(T_{12}=0)T=\frac{1}{2}\rangle$, $|(T_{12}=1)T=\frac{1}{2}\rangle$, and $|(T_{12}=1)T=\frac{3}{2}\rangle$.

APPENDIX B

In this appendix the functions $I^L_{N_B L_B, N_R L_R}(r)$ from the expression (33) are presented:

$$I^0_{00,00} = \left(\frac{27}{15+16\alpha_k b^2}\right)^{3/2}\exp\left\{-\frac{3r^2}{b^2}\frac{3+5\alpha_k b^2}{15+16\alpha_k b^2}\right\},$$

$$I^1_{00,11} = -I^0_{00,00}g\frac{r}{b},$$

$$I^0_{00,20} = I^0_{00,00}\sqrt{6}g\left(1-\frac{gr^2}{2b^2}\right),$$

$$I^2_{00,22} = I^0_{00,00}\sqrt{\frac{3}{5}}\frac{g^2r^2}{b^2},$$

$$I^1_{00,31} = -I^0_{00,00}\sqrt{10}\frac{g^2r}{b}\left(1-\frac{3gr^2}{10b^2}\right),$$

$$I^0_{11,11} = -I^0_{00,00}\sqrt{12}g\left(1-\frac{gr^2}{2b^2}\right),$$

$$I^2_{11,11} = -I^0_{00,00}\sqrt{\frac{6}{5}}\frac{g^2r^2}{b^2},$$

$$I^1_{11,20} = I^0_{00,00}5\sqrt{\frac{2}{3}}\frac{g^2r}{b}\left(1-\frac{3gr^2}{10b^2}\right),$$

$$I^1_{11,22} = I^0_{00,00}2\sqrt{\frac{10}{3}}\frac{g^2r}{b}\left(1-\frac{3gr^2}{10b^2}\right),$$

$$I^3_{11,22} = I^0_{00,00}3\sqrt{\frac{3}{35}}\frac{g^3r^3}{b^3},$$

$$I^0_{11,31} = -I^0_{00,00}2\sqrt{30}g^2\left(1-\frac{gr^2}{b^2}+\frac{3g^2r^4}{20b^4}\right),$$

$$I^2_{11,31} = -I^0_{00,00}\frac{2\sqrt{3}}{5}\frac{g^3r^2}{b^2}\left(7-\frac{3gr^2}{2b^2}\right),$$

$$I^0_{20,20} = I^0_{00,00}10g^2\left(1-\frac{gr^2}{b^2}+\frac{3g^2r^4}{20b^4}\right),$$

$$I^2_{22,20} = I^0_{00,00}\sqrt{\frac{2}{5}}\frac{g^3r^2}{b^2}\left(7-\frac{3gr^2}{2b^2}\right),$$

$$I^0_{22,22} = I^0_{00,00}4\sqrt{5}g^2\left(1-\frac{gr^2}{b^2}+\frac{3g^2r^4}{20b^4}\right),$$

$$I^2_{22,22} = I^0_{00,00}2\sqrt{\frac{14}{5}}\frac{g^3r^2}{b^2}\left(1-\frac{3gr^2}{14b^2}\right),$$

$$I^4_{22,22} = I^0_{00,00}3\sqrt{\frac{2}{35}}\frac{g^4r^4}{b^4},$$

$$I^1_{22,31} = -I^0_{00,00}\frac{4}{\sqrt{3}}\frac{g^3r}{b}\left(7-\frac{21gr^2}{5b^2}+\frac{9g^2r^4}{20b^4}\right),$$

$$I^3_{22,31} = -I^0_{00,00}\frac{27}{5}\sqrt{\frac{6}{7}}\frac{g^4r^3}{b^3}\left(1-\frac{gr^2}{6b^2}\right),$$

$$I^1_{20,31} = -I^0_{00,00}14\sqrt{\frac{5}{3}}\frac{g^3r}{b}\left(1-\frac{3gr^2}{5b^2}+\frac{9g^2r^4}{140b^4}\right),$$

$$I^0_{31,31} = I^0_{00,00}28\sqrt{3}g^3\left(1-\frac{3gr^2}{2b^2}+\frac{9g^2r^4}{20b^4}-\frac{9g^3r^6}{280b^6}\right),$$

$$I^2_{31,31} = I^0_{00,00}\frac{36}{5}\sqrt{\frac{3}{10}}\frac{g^4r^2}{b^2}\left(7-\frac{3gr^2}{b^2}+\frac{g^2r^4}{4b^4}\right),$$

where

$$g = \frac{4\alpha_k b^2 - 3}{15 + 16\alpha_k b^2}.$$

All the other functions can be developed using $I^L_{N_RL_R,N_BL_B} = (-1)^L I^L_{N_BL_B,N_RL_R}$.

[1] L. Ya. Glozman, N. A. Burkova, E. I. Kuchina, and V. I. Kukulin, Phys. Lett. B **200**, 983 (1988); L. Ya. Glozman, N. A. Burkova, and E. I. Kuchina, Z. Phys. A **332**, 339 (1989).

[2] A. Buchmann, Y. Yamauchi, and A. Faessler, Nucl. Phys. **A496**, 621 (1989); Y. Yamauchi, A. Buchmann, and A. Faessler, *ibid.* **A494**, 401 (1989); A. Faessler, A. Buchmann, and Y. Yamauchi, Int. J. Mod. Phys. E **2**, 39 (1993).

[3] I. T. Obukhovsky and A. M. Kusainov, Yad. Fiz. **47**, 494 (1988) [Sov. J. Nucl. Phys. **47**, 313 (1988)].

[4] I. T. Obukhovsky and A. M. Kusainov, Phys. Lett. B **238**, 142 (1990); A. M. Kusainov, V. G. Neudatchin, and I. T. Obukhovsky, Phys. Rev. C **44**, 2343 (1991).

[5] M. Oka and K. Yazaki, Prog. Theor. Phys. **66**, 556 (1981); **66**, 572 (1981); in *Quarks and Nuclei*, edited by W. Weise, International Review of Nuclear Physics Vol. 1 (World Scientific, Singapore, 1984), p. 489.

[6] A. Faessler *et al.*, Nucl. Phys. **A402**, 555 (1983).

[7] I. T. Obukhovsky and E. V. Tkalya, Yad. Fiz. **35**, 401 (1982) [Sov. J. Nucl. Phys. **35**, 230 (1982)].

[8] L. Ya. Glozman, V. G. Neudatchin, I. T. Obukhovsky, and A. A. Sakharuk, Phys. Lett. B **252**, 23 (1990).

[9] L. Ya. Glozman, V. G. Neudatchin, and I. T. Obukhovsky, Phys. Rev. C **48**, 389 (1993).

[10] L. Ya. Glozman, U. Straub, and A. Faessler, J. Phys. G (in press).

[11] P. Benz and P. Soding, Phys. Lett. **52B**, 367 (1974).

[12] H. J. Weber and H. Arenhovel, Phys. Rep. **36**, 279 (1978); A. M. Green, Rep. Prog. Phys. **39**, 1109 (1976).

[13] R. D. Amado, Phys. Rev. C **19**, 1473 (1979); A. S. Goldhaber, Nucl. Phys. **A294**, 293 (1978).

[14] E. W. Schmid *et al.*, Few-Body Syst. **5**, 45 (1988).

[15] V. G. Neudatchin, Yu. F. Smirnov, and N. F. Golovanova, Adv. Nucl. Phys. **11**, 1 (1979).

[16] O. F. Nemets, V. G. Neudatchin, A. T. Rudchik, Yu. F. Smirnov, and Yu. M. Tchuvilsky, *Nucleon Clustering in Light Nuclei and Multinucleon Transfer Reactions* (in Russian) (Naukova Dumka, Kiev, 1988).

[17] A. De. Rujula, H. Georgi, and S. L. Glashow, Phys. Rev. D **12**, 147 (1975).

[18] U. Vogl and W. Weise, Prog. Part. Nucl. Phys. **27**, 195 (1991).

[19] D. I. Dyakonov and V. Yu. Petrov, Nucl. Phys. **B272**, 457 (1986); D. I. Dyakonov, V. Yu. Petrov, and P. V. Pobylitsa, *ibid.* **B306**, 809 (1988).

[20] A. Valcarce, F. Fernandez, and A. Buchmann (unpublished).

[21] Z. Y. Zhang, A. Faessler, U. Straub, and L. Glozman (unpublished).

[22] N. Isgur and G. Karl, Phys. Rev. D **18**, 4187 (1978); **19**, 2653 (1979).

[23] F. E. Close, *An Introduction to Quarks and Partons* (Academic, London, 1979).

[24] I. V. Kurdyumov, Yu. F. Smirnov, K. V. Shitikova, and S. H. El Samarae, Nucl. Phys. **A145**, 593 (1970).

[25] N. Hamermesh, *Group Theory and Its Application to Physical Problems* (Addison-Wesley, Reading, MA, 1964).

[26] W. Weyrauch and H. J. Weber, Phys. Lett. B **171**, 13 (1986).

[27] A. Buchmann, E. Hernandez, and K. Yazaki, Phys. Lett. B **269**, 35 (1991).

[28] C. S. Kalman and B. Tran, Nuovo Cimento A **102**, 835 (1989); **104**, 177 (1991).

[29] Yu. F. Smirnov and Yu. M. Tchuvilsky, J. Phys. G **4**, L1 (1978); E. V. Kuznetsova, Yu. F. Smirnov, R. M. Al-Hovari, and Yu. M. Tchuvilsky, Izv. Akad. Nauk Kaz. SSR (Alma-Ata) **1**, 3 (1979).

[30] V. A. Matveev and P. Sorba, Nuovo Cimento A **45**, 257 (1978).